AD-A178 761 SIGNATURES FROM IN-SITU LIGHT SCATTERING OF NON-HOMOGENEOUS NON-SPHERICAL (U) GEORGIA INST OF TECH ATLANTA SCHOOL OF GEOPHYSICAL SCIENCES A COLETTI

1/1

UNCLASSIFIED 06 FEB 87 ARO-21016 1-GS DAAG29-84-K-0115 F/G 20/6 NL

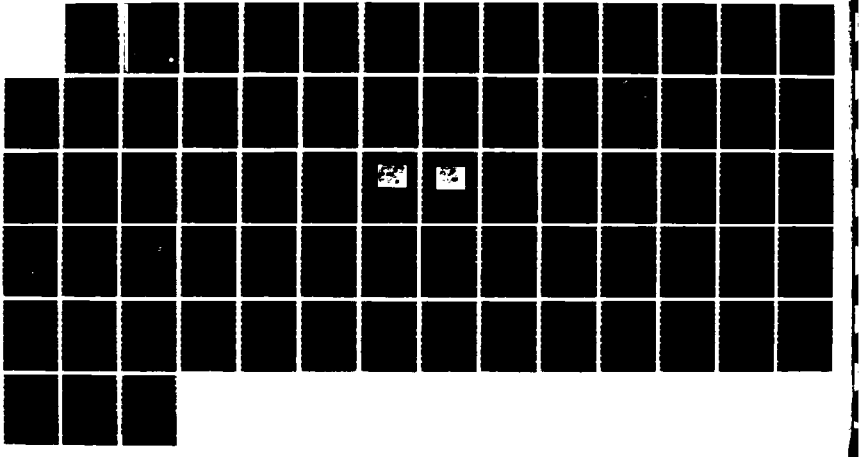

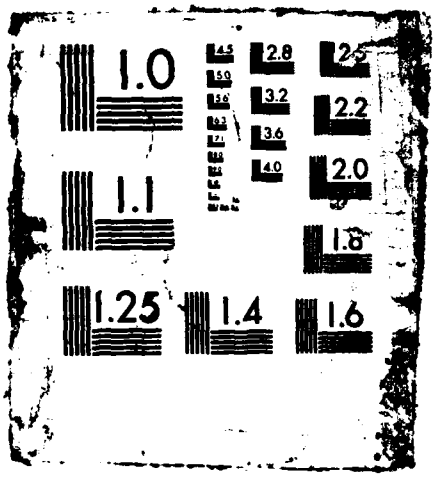
1.0
1.1
1.25
1.4
1.6
2.8
3.2
3.6
4.0
2.2
2.0
1.8

FINAL REPORT

SIGNATURES FROM IN-SITU LIGHT SCATTERING OF NON-HOMOGENEOUS NON-SPHERICAL PARTICLES

By

Alessandro Coletti

February 6, 1987

Prepared for

U.S. ARMY RESEARCH OFFICE

Under

Contract Number DAAG29-84-K-0115

GEORGIA INSTITUTE OF TECHNOLOGY
A UNIT OF THE UNIVERSITY SYSTEM OF GEORGIA
SCHOOL OF GEOPHYSICAL SCIENCES
ATLANTA, GEORGIA 30332

1987

SIGNATURES FROM IN-SITU LIGHT SCATTERING OF NON-HOMOGENEOUS NON-SPHERICAL PARTICLES

FINAL REPORT

Alessandro Coletti

February 6, 1987

U.S. ARMY RESEARCH OFFICE

Contract Number DAAG29-84-K-0115

SCHOOL OF GEOPHYSICAL SCIENCES
GEORGIA INSTITUTE OF TECHNOLOGY
ATLANTA, GEORGIA 30332

UNCLASSIFIED

SECURITY CLASSIFICATION OF THIS PAGE (When Data Entered)

REPORT DOCUMENTATION PAGE		READ INSTRUCTIONS BEFORE COMPLETING FORM
1. REPORT NUMBER ARO 21016.1-GS	2. GOVT ACCESSION NO. N/A	3 RECIPIENT'S CATALOG NUMBER N/A
4. TITLE (and Subtitle) Signatures from in-situ light scattering of non-homogeneous non spherical particles.		5 TYPE OF REPORT & PERIOD COVERED Final JAN 31,1987 July 1, 1984 ~~Sept 30, 1986~~ 6 PERFORMING ORG. REPORT NUMBER
7. AUTHOR(s) Alessandro S. Coletti		8. CONTRACT OR GRANT NUMBER(s) DAAG 29-84-k-0115
9. PERFORMING ORGANIZATION NAME AND ADDRESS School of Geophysical Sciences Georgia Institute of Technology Atlanta, Georgia 30332		10. PROGRAM ELEMENT, PROJECT, TASK AREA & WORK UNIT NUMBERS
11. CONTROLLING OFFICE NAME AND ADDRESS U. S. Army Research Office Post Office Box 12211 Research Triangle Park, NC 27709		12. REPORT DATE December 15, 1986 13. NUMBER OF PAGES
14. MONITORING AGENCY NAME & ADDRESS(if different from Controlling Office)		15. SECURITY CLASS. (of this report) Unclassified 15a. DECLASSIFICATION/DOWNGRADING SCHEDULE

16. DISTRIBUTION STATEMENT (of this Report)

Approved for public release; distribution unlimited.

17. DISTRIBUTION STATEMENT (of the abstract entered in Block 20, if different from Report)

NA from 16

18. SUPPLEMENTARY NOTES

The view, opinions, and/or findings contained in this report are those of the author(s) and should not be construed as an official Department of the Army position, policy, or decision, unless so designated by other documentation.

19. KEY WORDS (Continue on reverse side if necessary and identify by block number)

→ Light scattering, aerosol particles, laser measurements, numerical inversions

are enclosed ↑

20. ABSTRACT (Continue on reverse side if necessary and identify by block number)

The research performed under this program has focused on studying the angular light scattering of monodisperse quasi spherical non homogeneous particles. For that purpose ~~we had to develop~~ specific laboratory techniques suitable for the generation of these particles and for properly collecting the data. For comparing the measurements with the light scattering theories for spheres and spheroids we have formulated a new kind of algorithm that is innovative in many aspects and has useful application. The method might be advantageous for

DD FORM 1 JAN 73 1473 EDITION OF 1 NOV 65 IS OBSOLETE

UNCLASSIFIED

SECURITY CLASSIFICATION OF THIS PAGE (When Data Entered)

(20. ABSTRACT cont.)

inversions of physical parameters from experimental data, and for estimating their statistical significance. Keywords: [illegible] fractal [illegible]

TABLE OF CONTENTS

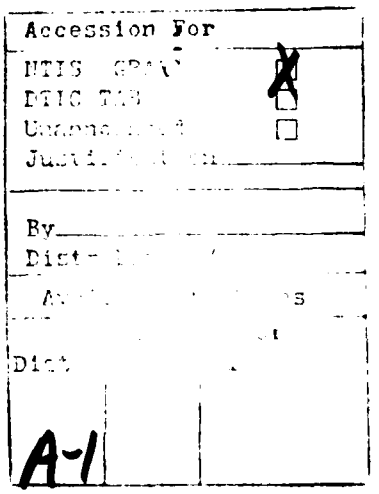

PROGRAM OVERVIEW

The major objective of this research is to further develop numerical methods for the analytical treatment of angular light scattering from randomly oriented non-spherical non-homogeneous particles. This requirement has been achieved with the development of the numerical method described in the following paragraphs which is the result of our study performed on laboratory generated light scattering data. We feel that the approach we are suggesting has many innovative aspects, and can be used in many practical problems.

During the work we have devised laboratory techniques (described in Appendix A) for generating the data, and we have performed a feasibility study on a new kind of light scattering instruments (described in the Appendix B) that performs angular scans without using moving optical parts. Homogeneous spherical particles made with mixed solutions of ammonium sulfate-methylene blue and ammonium sulfate- nigrosine dye have been used as a reference. Inhomogeneous particles have been made by mixing ionic salts with gold and silver colloids at various stages of their nucleation. Metallic colloids of silver and gold have been chosen because they nucleate in relatively narrow size distributions and relatively small uncertainties exist in the values of the refractive index. Some typical results of angular light scattering measurements obtained with these chemical solutions are reported in Appendix C of this note.

We have confirmed that the angular light scattering measurements taken every 5° in the angular interval between 10 and 170°, could not be interpreted with the Lorenz-Mie theory for homogeneous spherical particles. However, the application of light scattering theory for spheroids (with the EBCM program kindly provided to us by Dr. Peter Barber) turned out to be cumbersome and of doubtful use. In fact in the few cases where the particle sizes were small enough to permit practical applications of the EBCM theory, limitations existed on the statistical significance of the particle sizes and axial ratios as obtained with the electron scanning microscope, and on the values of the effective refractive index applicable to the mixtures.

Consequently, a different approach has been attempted where the optical measurements are analyzed for their information content in terms of particle composition and shape. Basically the method consists of calculating the Legendre polynomial series fitting the experimental data. The set of these coefficients can be compared with theoretical sets calculated for different properties of the particles. The advantage of the method, against standard inversion methods, arises mostly from the more compact representation of the phase functions allowed by the use of the Legendre polynomials. In what follows we report a few examples of how the proposed method may be applied in practice.

1. INTRODUCTION

Angular light scattering measurements of natural and laboratory generated aerosols contain information on the size, chemical composition and shape of the particles. Nevertheless, up to the present date, the numerical inversion techniques applied to experimental data have been based on the Lorenz-Mie theory for spherical homogeneous particles (Ferrara et al., 1970; Grams et al., 1974; Quenzel, 1970; Takamura and Tanaka, 1985). To the best of our knowledge, the only numerical study on the possibility of inferring particle shapes from simulated light scattering data has been made by Heintzenberg and Welch (1982). These authors show that even though the light scattering contains information on the particle shape, still its retrieval is practically impossible if the assumption is made that no previous knowledge of particle shape is available.

The differences in the light scattering by spheres and spheroids have been described by Yamamoto and Tanaka (1969) and Barber and Yeh (1975). They have shown that basic quantitative and qualitative differences exist even though the position of maxima and minima in both scattering coefficient and asymmetry parameter (proportional through a numerical constant to the first coefficient of the Legendre polynomial series) for spheroidal and spherical particles have some qualitative similarities. Important contributions to the numerical capability for computing the light scattering properties of non-spherical particles have

been achieved by Barber and Liou (see e.g. Liou et al. 1983). They also focused their attention on some of the particle characteristics that can facilitate their recognition in experiments.

Basically, the data analysis described here provides criteria for the recognition of non-spherical particles from light scattering data. The method follows from calculations made by Chu and Churchill (1955) on the Legendre polynomial expansion of the Lorenz Mie theory and discussions by Van de Hulst (1980). Interest in the study of the Legendre polynomial coefficients originates both from their advantageous mathematical properties and from their physical meaning in the spherical harmonics expansion of the scattered field.

Fig. 1 shows some examples of Legendre polynomial coefficients computed for spherical particles of various refractive indices as a function of one half of their phase shift ρ ($\rho=4\pi r/\lambda\ [m-1]$). The various curves represent the coefficients from the 1st to the 19th order polynomial. Fig. 1 a) is for a refractive index, m=1.3, b) for m=1.4, c) for m=1.5, and d) for a light absorbing particle with m=1.5 - i0.5. The compactness of this kind of representation can be easily appreciated when it is realized that each of these figures describes all the major features of the phase functions in the interval under consideration. The resolution used in the figures shows some of the characteristics of the Legendre polynomial coefficients that

Van de Hulst could not determine from Chu and Churchill calculations. Namely, the maxima and minima of the coefficients appear to occur at similar values of phase shift until the order of the coefficient is larger than x-1/2 ($x=2\pi r/\lambda$); for higher values of the order, their position moves with an almost power law toward larger values of ρ as the order of the coefficient increases.

Numerically, the Legendre polynomial coefficients of both spherical and spheroidal particles can be easily obtained from the existing numerical codes since the Legendre polynomials are readily available as part of these of programs. They can instead be estimated experimentally from angular light scattering measurements, but only under specific experimental conditions. For a given phase function, $\phi(\mu)$, the n-th order coefficient, ω_n, is given by:

$$(2n+1)\ \omega_n = 2 \int_{-1}^{+1} \phi(\mu) P_n(\mu) d\mu \qquad (1$$

where $P_n(\mu)$ is the n-th order Legendre polynomial and $\mu=\cos\ \Theta$. If we have N light scattering measurements, V_i (i=1,..,N), performed at angles Θ_i, we can compute N parameters g_n:

$$g_n = \sum_{1}^{N} {}_i V_i w_i P_n(\mu_i) \qquad (2$$

where w_i are suitable weights.

For a measured phase function ϕ we can write:

$$\phi = \sum_{0}^{M} \omega_n P_n \quad M<(N+1)/2 \qquad (3$$

So that it results also:

$$g_n=(2n+1)\omega_n+\epsilon \qquad (4$$

if Gauss Jacobi quadrature has been used in eq. 2 and ϵ is the experimental error on the estimate of g_n. Then, for instance by looking at the numerical tables (e.g. Abramovitz and Stegun, 1965), a 12 points quadrature has the first and last experimental points at light scattering angles of about 11° and 169°; these are minimum and maximum angles close to those generally used in the experiments. This means that, at the best, eq. 2 can be properly applied only in the case of phase functions that can be represented reasonably well by a 6th order polynomial (that is for particles in Fig. 1c with phase shift lower that 4). This result is analogous to the conclusion reached by Mugnai and Wiscombe (1986) when they analyzed the truncation errors introduced in the experimental estimates of the asymmetry parameter for spherical and spheroidal particles with various characteristics. In fact, Eq. 5 would give their same results if applied for n=1 in the case of an instrument that precisely

measures light scattering phase functions within a given angular interval. For larger particle sizes where the contributions due to polynomials of higher order become sensible, the parameters g_n measured in a limited interval of angles can not be any longer equated to the w_n's. Therefore we can compute only the quantities:

$$g_n = \int_{\mu_1}^{\mu_2} \phi P_n d\mu + \epsilon = \sum_{1}^{N} {}_i \omega_i \phi_i P_n + R + \epsilon \qquad (5$$

where μ_1 and μ_2 are the cosines of the minimum and maximum measurable angles and R the remainder. It will be shown in the next section that even in this case there is a usable information content of the g_n coefficients of the various orders so that, under suitable experimental conditions, it is still possible to overcome some of the drawbacks described by Mugnai and Wiscombe and by Heintzenberg and Welch.

In the meantime, we can observe that independently of whether eq. 2 or eq. 5 are satisfied, the optimized Legendre polynomial series of experimental data provides the best interpolation method of the measurements independent of particle shapes in the least square sense. This interpolation is preferable to the one we have previously proposed (Coletti, 1984)

where interpolation of the forward light scattering of experimental phase function of quasi spherical particles was performed using diffraction theory, and where the backward scattering, important for remote sensing measurements, was treated empirically.

2. APPLICATIONS

2.1 The direct problem

To illustrate the practical advantages presented by the representations in terms of g_n coefficients, let us consider the following problem: we want to perform angular light scattering measurements to distinguish between monodisperse spherical particles with real refractive index 1.5 from particles with complex refractive index 1.5 -i0.01 in the size parameter range between 3 and 20. We want to estimate the best angles to use for measurements where no dependable measurements can be taken at angles smaller than 10° and greater than 170°.

For the purpose we suppose that the relative experimental error, ϵ, has a statistical distribution with variance proportional to the true values of the V's, V*. Then we can see that (dropping the weights in the summation for simplicity):

$$\sum_{1}^{N}{}_i \; V_i P_{n,i} = \sum_{1}^{N}{}_i \; V^*_i P_{n,i} + \epsilon \sum_{1}^{N}{}_i V^*_i \; P_{n,i}$$

$$\equiv (1+\epsilon)\; g_n^* \qquad (6$$

That is, under our assumption, the relative errors in the g_n are

the same for any n. Therefore in Fig. 2, where the relative variations of the g_n coefficients in the two cases of the light absorbing and non light absorbing particles are shown (for the refractive indices 1.5 and 1.5 -i0.01), the two kinds of particles will be indistinguishable whenever the relative differences of all the considered coefficients will be simultaneously smaller than the errors. Fig. 2 has been drawn by computing the g's for the two kinds of particles in the angular interval between 10 and 170°. The isopleths have only an illustrative purpose since the functions $g_n(x)$ do not describe a continuous surface. Following the example under discussion, we can estimate that performing measurements with a precision of 10% we need to estimate g_n coefficients up to the 5th order to discriminate light absorbing and non light absorbing particles in the size parameter interval between 6 and 17. In fact, for any of those particles, Fig .2 shows that there is at least one of the first five coefficients that differs in the two cases for more than the expected experimental error.

Numerical procedures, analogous to the one just described, can be used to obtain the sensitivity of instruments to detect significant variations in the particle properties. With the traditional method quantities such as:

$$x^2 = \sum_{1}^{N}{}_i \; (1-\phi'_i/\phi''_i)^2 \qquad (7$$

would have been evaluated to estimate if the differences existing between two phase functions, ϕ' and ϕ'', are sufficiently large to be detected. No information would have been obtained on the differences existing between the spherical harmonic structures of the phase functions, therefore no indication would become available with this latter method on how to optimize the number and the position of the angles for the measurements.

If needed, evaluations similar to those made in Fig. 2 can be made also in a variety of other cases where it is desired to estimate the capability to resolve between particles of different shapes, composition, aggregation state, or polydispersion.

2.2 The Inverse Problem

We now consider the simple exercise where we want to determine with the Lorenz-Mie theory for spherical homogeneous particles the effective refractive index of a monodisperse aerosol of sodium chloride particles. The numerical implications of the method for general inversions will be discussed later.

The Sodium Chloride particles have a quasi-spherical shape and hollow internal structure as discussed by Coletti (1982), the light scattering phase function for a particle of size parameter $x = 5$ is shown in Fig. 3. The squares in the figure represent the results of the measurements. The continuous line in the figure represent the results of a best fit obtained with the Lorenz-Mie theory for a size parameter 5 and a refractive index 1.54. We

can see in the figure that the fit is not totally satisfactory, and we want to investigate whether there exists an effective, purely real, value of refractive index that can provide a better fit.

We compute the optimized Legendre polynomial series that best fits the experimental values, and we compare the coefficients with those of the best fitting sphere in the two cases of refractive index 1.54 (refractive index of salt) and 1.3. This latter value of the refractive index has been obtained applying the simple volume mixing of the refractive index of vacuum and salt in the ratio discussed in our previous work. Fig 4 shows the coefficient of the optimized series as computed from the measurements (squares) and the line boundaries determined by the two theoretical spherical particles at the two indices of refraction (upper continuous line, m=1.54; lower continuous line, m=1.3). The vertical line in the figure has been drawn for the value of n for which grazing rays are given by the localization principle. We can observe that the experimental coefficients have values that shifts between the two boundaries. Therefore, considering Fig. 4 and the results discussed in Fig 1 a,b,c, we can conclude not only that neither value of the refractive index satisfies the requirements of a good fit, but also that a good fit does not exist for any other value of refractive index in the considered interval. Therefore, the Lorenz-Mie theory for spherical homogeneous particles with x=5 and m=1.54 provides a

fit that is dependable only up to the 1st order of the polynomial expansion in the Legendre series, and the particles with m=1.3 fit the coefficients with order between 7 and 10. Nevertheless, these features are specific for sodium chloride particles of this size, and it can be seen in Fig. 2, Appendix C, that different behavior is exhibited for other particle sizes.

In more a general numerical inversion problem, a minimum chi-square is generally searched assuming that each measured value V_i can be represented as a linear combination of a number concentration of particles (having given size, refractive index, shape) and their theoretical values of light scattering at the various angles, that is, using matrix notations:

$$\vec{V} = \|A\| \vec{c} \qquad (8$$

where $\vec{c}$ is the array of the particle concentration, and the elements a_{ij} of the matrix A are the theoretical values of the light scattering of the particle of size x_j at the angle θ_i:

$$a_{ij} = \phi(x_j;\theta_i) \qquad (9$$

Where:

$$\phi(x_j;\theta_i) = \sum_{o}^{\infty} w_m P_m \qquad (10$$

The measurement array has, by definition, all the Legendre polynomial coefficients of order higher than the total number of

the measurements, N, equal to zero. Then, it is easily seen that this portion of the series

$$\sum_{N}^{\infty} {}^{m} w_m P_m$$

coming from the theoretical values of the ϕ's, and normally included in the calculations made so far (see e.g. Grams et al. 1974), can lead to erroneous results under unfavorable conditions. In fact, in the form of eq. 4 this quantity escapes any theoretical analysis of aliasing and of the estimates of the remainder of the series. In contrast, analysis with the Legendre polynomial along with a suitable quadrature formula (see e.g. Scarborough, 1966) permits quantitative estimates of these latter quantities.

We can briefly discuss the direct use of the coefficients g_n in the case of a general linear inversion. Substituting eq. 4 in eq. 8 we can write:

$$a_{ij} = \sum_{0}^{M} {}_{n} \omega_n(x_j) \; P_n(\theta_i) \qquad (11$$

and accordingly introduce the matrices Π and Ω:

$$\|A\| = \|\Pi\| \; \|\Omega\| \qquad (12$$

where the generic element ω_{ik} of the matrix Ω is

$$\omega_{jk}=\omega_k(x_j) \qquad (13$$

and the generic element of the matrix Π is:

$$\pi_{ni}= P_n(\theta_i) \qquad (14$$

Multiplying both sides of eq. 8 by the matrix Π^T and by the matrix $\|\Pi^T\Pi\|^{-1}$ we obtain:

$$\|\Pi^T\Pi\|^{-1}\|\Pi^T\| \vec{V} = \|\Omega\| \vec{c} \qquad (15$$

But the left hand side of the equation is basically the same of eq. 2, then

$$\vec{g}= \|\Omega\| \vec{c} \qquad (16$$

Eq. 16 is similar to eq. 8 and can be solved with the usual methods (S. Twomey, 1977; G. Backus and F. Gilbert, 1970). The use of this equation instead of eq. 8 has the further advantage that the values of the elements ω_{ij} can be expected to cover a range of numerical values narrower than those assumed by the corresponding elements A_{ij}. It can be anticipated that this should give some numerical advantage during the calculation of the inverse matrix. In fact, the elements a_{ij} that represent the values of the phase function of a particle x_i at the angle θ_j, often span three or four decades, and this makes cumbersome the already numerically delicate inversion of the matrix A.

The parameters obtained by the numerical inversions, can be compared with the original experimental data in a fashion totally similar to that described in the case of monodisperse non-homogeneous particles. Therefore similar insights into the nature of particle polydispersion should be possible.

3. CONCLUSIONS

The purpose of the examples discussed in this note is to illustrate some applications where the series expansion of phase functions in spherical harmonics can be applied. Basically, we have shown how it is possible to analyze and describe differences existing between phase functions, or classes of phase functions, more efficiently then by comparing them point by point. We have shown how this can be useful during analysis of light scattering data of particle mixtures and to verify up to what extent the hypothesis in use properly approximate the physical or chemical state of the particles.

We feel that the use of spherical harmonics for studying the light scattering properties of particles has not been sufficiently explored. In fact the methods described here are just very simple consequences of the fact that the spherical harmonics coefficients permits a more compact representation of particle phase functions numerically and graphically.

In this paper objective criteria for optimizing experimental procedures of angular light scattering have been provided for the first time.

4. LIST OF TECHNICAL REPORTS PUBLISHED

Coletti, A., 1984, A possible experimental application of some properties of the first expansion coefficients of the phase function, CRDC, SP-85007.

5. LIST OF PARTICIPATING PERSONNEL

Dr. A. S. Coletti (PI)
Dr. G. W. Grams
Dr. E. M. Patterson
Mr. C. M. Wyman

Graduate Students:

Mr. Alan Chu
Mr. Xiao Jingwei

References

M. Abramovitz, and I.A. Stegun, Dover, NY, 1965

A. Coletti, 1984. Aer. Sci. and Tech., 3, 39.

G. Backus, and F. Gilbert, 1970, Philos. Trans. R. Soc. London, 266, 625

P. Barber, and c. Yeh, 1975. Appl. Opt., 14, 2864.

C.M. Chu, and S.W. Churchill, 1955. J. Opt. Soc. Am., 45, 958.

R.Ferrara, G. Fiocco, and G.Tonna, 1970. Appl. Opt., 9, 2517.

G.W. Grams, I.H. Blifford, Jr., D.A. Gillette, and P.B.Russel, 1974. J. Appl. Meteorol., 13, 459.

J. Heintzenberg, and R.M. Welch, 1982. Appl. Opt., 21, 822.

K.N. Liou, Q. Cai, P.W. Barber, and S.C. Hill, 1983. Appl. Opt., 22, 1684.

A. Mugnai, and W.J. Wiscombe, 1986, Appl. Opt., 25, 1235.

Quenzel, 1970. J. Geophys. Res. 75, 2815.

J.B. Scarborough: Numerical Mathematical Analysis, John Hopkins Press, 1966.

G. Yamamoto and M. Tanaka, 1969. Appl. Opt. 8, 447.

T. Takamura and M. Tanaka, 1985. Met. Soc. Japan Jour., 63, 969.

S. Twomey: Introduction to the Mathematics of Inversion in Remote Sensing and Indirect Measurements, Elsevier, 1977.

H.C. Van de Hulst: Multiple Light Scattering, Academic Press, 1980, p318.

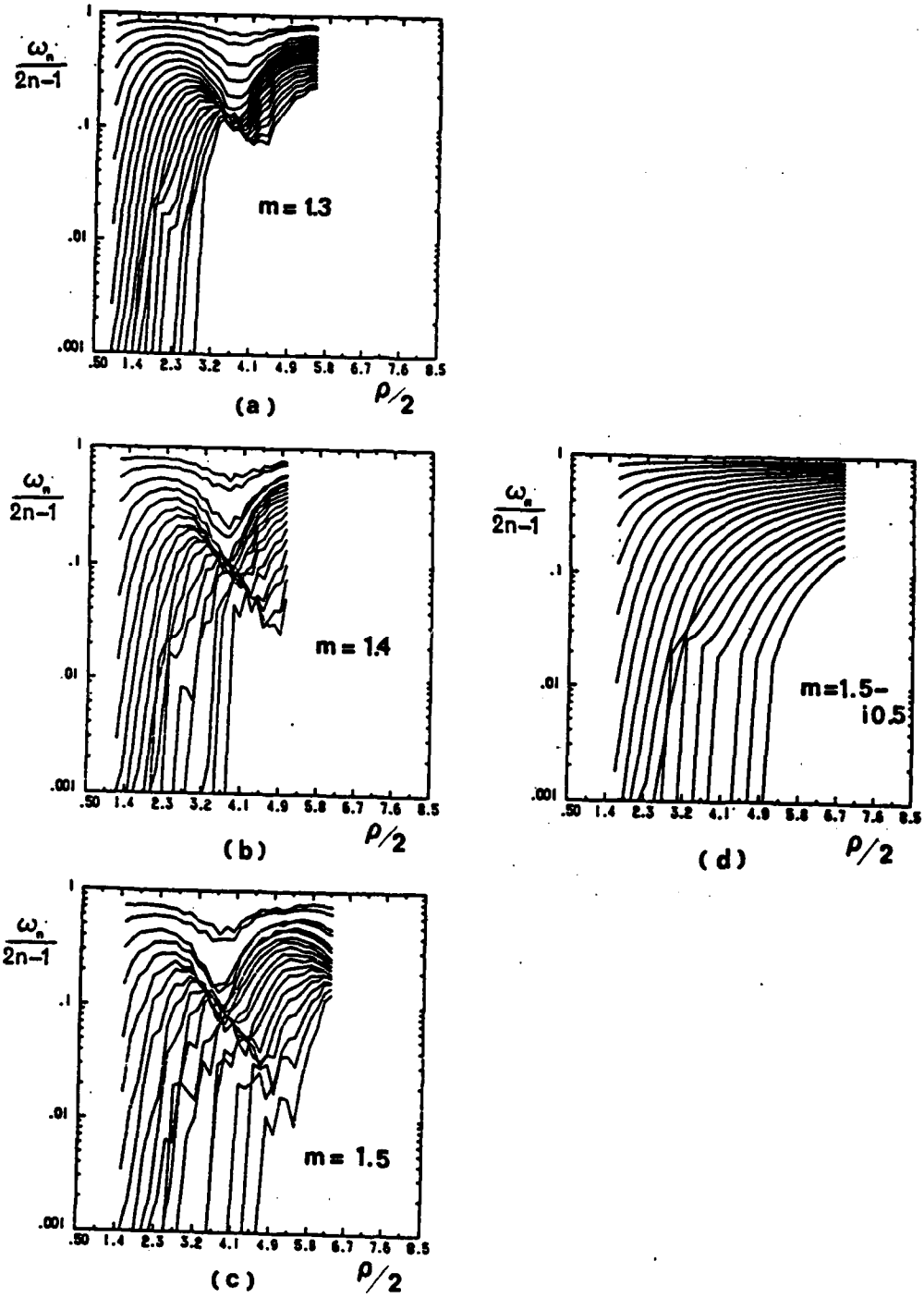

Fig. 1 - Legendre polynomial coefficients for various spherical particles as function of one half of the phase shift ρ (=2x[m-1]): a) refractive index 1.3; b) refractive index 1.4; c) refractive index 1.5; c) refractive index 1.5 -i 0.5. Note in the figure how the minima occurring for the phase shifts near 7 suddenly start shifting toward higher values when the order of the coefficients becomes higher then 7.

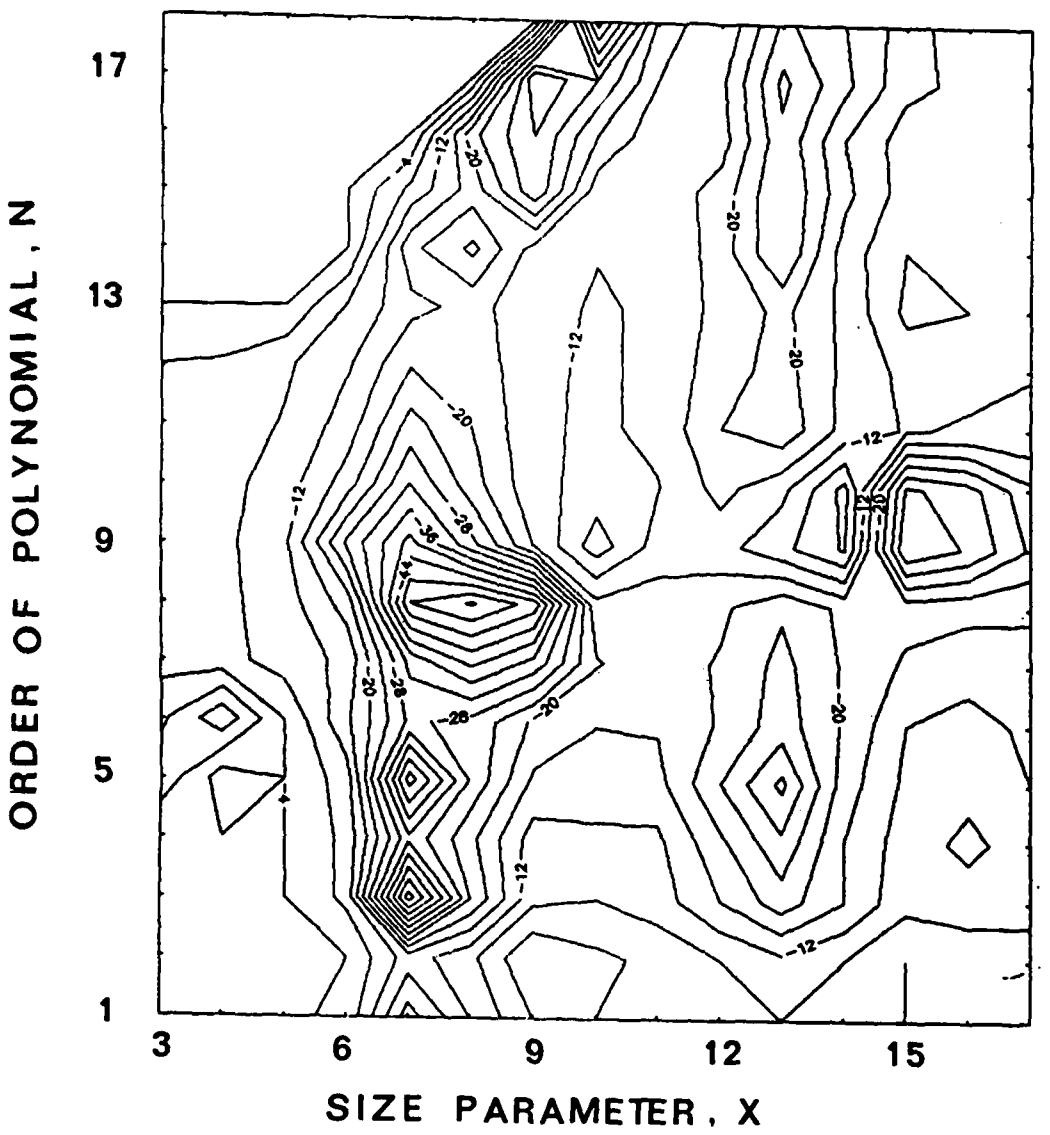

Fig. 2 - Line contours in a table reporting relative variations of the Legendre polynomial coefficients of various orders computed for different size parameters of light absorbing and non light absorbing spherical particles (m=1.5 -i0.1 and 1.5).

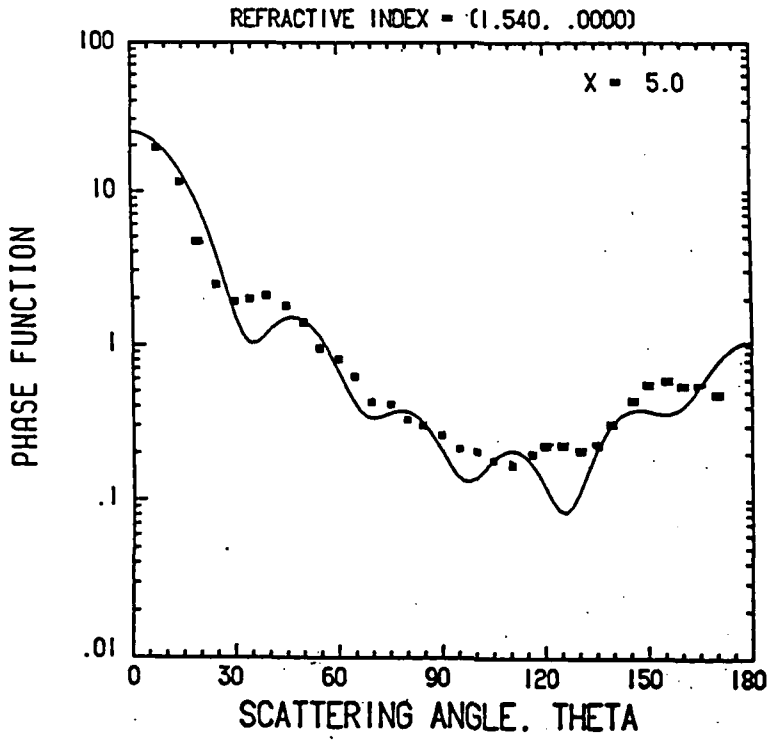

Fig. 3 - Normalized phase function measured on Sodium Chloride particles of size parameter 5 (squares) compared with spherical particles of same size and refractive index 1.54.

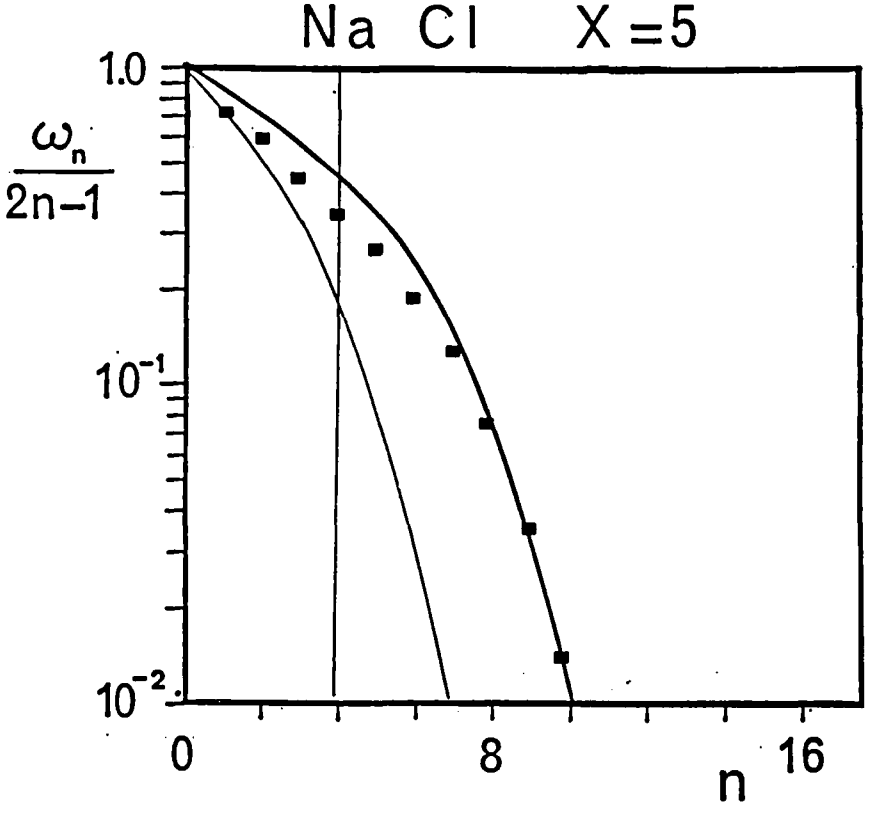

Fig. 4 - Comparison of the Legendre polynomial coefficients as computed from the measurements in Fig. 3 and the corresponding values obtained for spheres of size parameter 5 and refractive index 1.3 (lower curve)and 1.54 (upper curve). The theoretical values of the ω_n had been artificially connected with a continuous line to improve the clarity of the figure. The vertical line for n=4 indicates the order of the grazing rays as given by the localization principle.

APPENDIX A

AEROSOL COMPOSITION

To measure the light scattering properties of non-spherical particles and, separately, of non-homogeneous particles we used the Berglund Liu monodisperse aerosol generator that delivers particles with an almost monodisperse mass distributions.

Non-spherical particles have been used to test the light scattering theories for spheroidal particles (mostly the EBCM - extended boundary condition method - for spheroids) on irregularly shaped randomly oriented particles. To generate particles with the desired characteristics we had to develop new methods. In fact we could not use the usual methods of drying droplets containing ions with strong polar bonds in solution, because these particles often present sharp edges (e.g. Leong, 1985) and are unsuitable for the problem we had to investigate. During the measurements we have used mixtures of ionic salts, like ammonium sulfate or sodium chloride, and organic dyes, such as methylene blue and nigrosine dye. The results we have obtained using these mixtures indicated that these solutions when evaporated at the appropriate speed, yield smooth non-spherical aerosol particles. In our case, the speed of evaporation was controlled by varying the percentile of alcohol present in the solvent. The microphotograph reported in Fig. 1 shows as example particles of sodium chloride and nigrosine dye (mixed in equal parts in a solvent 50%-50% water and methanol). Fig 2 shows

anologuous results obtained with nigrosine dye and ammonium sulfate (mixed in a solvent 75% methanol-25% water).

Quasi-spherical particles containing homogeneous distribution of light absorbing particles (with size much smaller than the wavelength) have been chosen to study the applicability of the mixing rules for the refractive index. We have tested mixtures of metallic colloids and ionic salts and we have excluded particles containing carbon or soot particles. In fact, properly prepared Silver and Gold colloids are formed by narrow size distributions of spherical particles. The refractive index of these metals has been carefully studied and the optical properties of the colloids have been extensively described and discussed in the open literature.

Gold colloids have been obtained using procedures described by Turkevich et al (1951). A very narrow size distribution of small particles is obtained from the reaction of sodium citrate and chlorauric acid; this colloid is subsequently "developed" adding hydroxylamine hydrochloride that further coagulates metallic gold on the existing nuclei. This two step process produces a well defined narrow size distribution of spherical gold particles of the desired size but has a low yield since it is leaving a large fraction of gold in ionic form. The reaction between chlorauric acid and citric acid has been used for his high yield in gold particles even though the particle size distribution and shape were not well defined as in the previous case.

With the reaction with the sodium citrate, we have obtained

a distribution of spheres centered at about 15nm. In the reaction with the citric acid a broad distribution of spheres and triangular plates in the size range within 10-50 nm has been obtained.

Silver colloids have been produced with the reaction that has been studied among others by Von Raben et al. (1984). This reaction occurs at 0°C between silver nitrate and sodium borohydrade; the nucleation process has an high yield in spherical particles with narrow size distribution around 25 nm diameter with a 20% deviation. A good quality outcome from this reaction critically depends on the temperature applied during the process and few attempts have been necessary to produce a clear red-brownish sol of good quality stable with time.

These metallic colloids have been used with the vibrating orifice generator replacing the filter size suggested by the manufacturer (0.05 μm pores) with 1 μm pores filters. These filters have been found to suitably retain the coarser particles while allowing the majority of the particles with the specified diameter to pass through. In fact no significant change in the optical density of sample solutions could be detected before and after filtration.

Unfortunately, the analysis at the electron scanning microscope of the aerosol sampler collected on filters during the measurements, gave negative results in the case of colloidal solutions. In fact, these particles totally lost their original shape during the impact with the filter. Nevertheless, some of these microphotographs allowed us to estimate the mentioned

approximate size of the metallic particles forming the colloid.

For the final solutions, we used the mixtures listed in the following Table IA that lists concentrations, type of solvents used, and approximate size of the particles obtained from the vibrating orifice generator after evaporation of the dilutants.

The size of the particles listed in the table has been obtained estimating, whenever possible, the position of the first minimum in the measured forward light scattering and applying the formula derived from the diffraction theory of light, $x = 3.85/\sin 3$.

TABLE IA

Mixture Type	Reaction	Concentration	X	Fig Number (Appendix C)
Solvents: 50% Water	N/A	6.7×10^{-4}	12.6	1a
50% Ethanol		6.7×10^{-4}	11	1b
Solution		5.3×10^{-5}	7.8	1c
Sodium Chloride*		6.3×10^{-5}	5	1d
Nigrosine Dye (75%)	N/A	$Co=8.5 \times 10^{-4}$	8.7	3a
Ammonium Sulfate (25%)		Co/2	8.2	3b
Solvents: 75% Methanol		Co/4	8.1	3c
25% Water		Co/8	7.9	3d
		Co/16	6.2	3e
		Co/64	6.4	3f
		Co/128	3.9	3g
Chlorauric Acid/Sodium Citrate	Ref 3a	$Co=5.5 \times 10^{-4}$	-	-
Standard Solution		Co/4	9	4a
Solvents: 50% Ethanol		Co/8	6.7	4b
50% Water		Co/16	6.7	4c
Chlorauric Acid	Ref 3a	$Co=4.3 \times 10^{-4}$		
Citric Acid		Co/2		5a
Solvents: 50% Ethanol		Co/4		5b
50% Water				
Silver Nitrate	Ref 3a	$Co=8 \times 10^{-4}$		
Sodium Borohydrade		Co/2	13	6a
Solvents: 50% Ethanol		Co/4	11	6b
50% Water		Co/8	-	6c
		Co/8	9	6d
		Co/32	6	6e
		Co/64	5.4	6f

*Measurements performed during a previous research and reported here for the analysis in Legendre polynomial coefficients.

References

1A) Leong CRDC-DP-85007, p. 85, June 1985.

2A) K.U. Von Raben, R.K. Chang, B.L. Laube, and P.W. Barber. Jour. Phys. Chem. 1984, 88, 5290.

3A) J. Turkevich, P. Cooper Stevenson, and J. Hillier, Discussion of the Faraday Society, 11, 1951, p. 55.

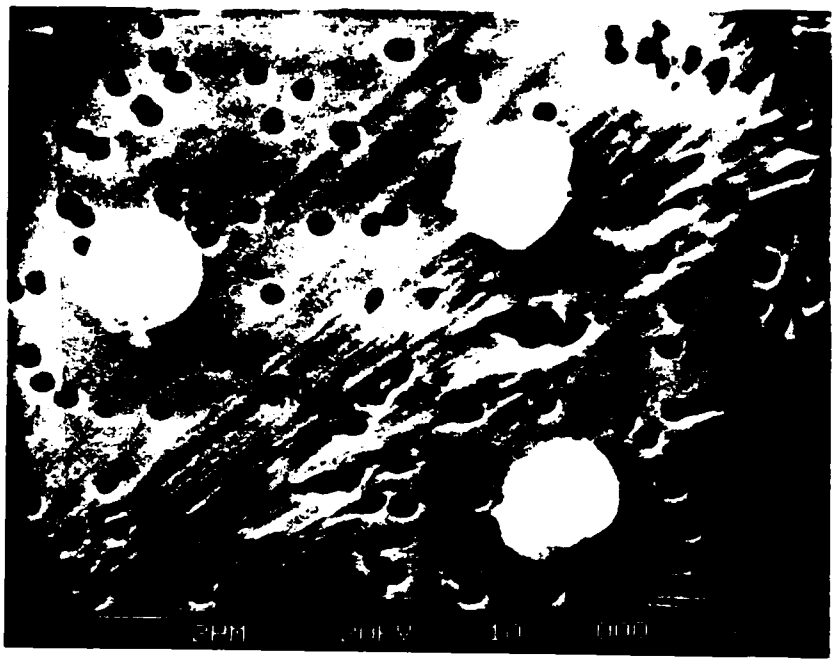

Fig 2 - Microphotograph of sample aerosol containing nigrosine dye and 25% ammonium sulfate

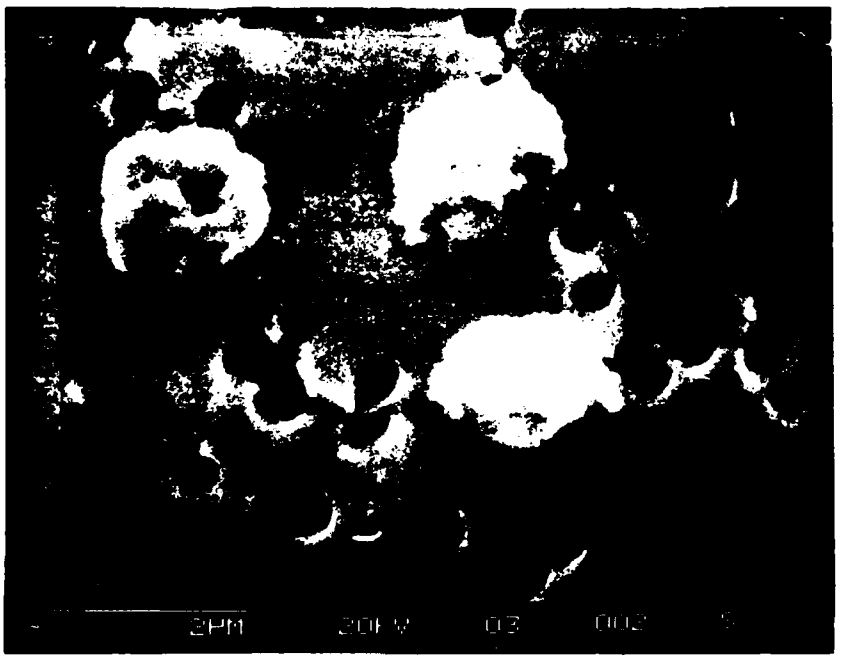

Fig 1 - Microphotograph of sample aerosol containing sodium chloride and 25% nigrosine dye

APPENDIX B

FISHEYE POLAR NEPHELOMETER

During the last few years, various designs for instruments capable of simultaneously measuring the light scattering of aerosols at different angles have been proposed. Reported in this note are some data relative to a preliminary study performed on a specific kind of such an instrument that uses a fisheye lens as a basic optical element.

Measurements made comparing a prototype of this instrument with another instrument already tested will be discussed on the basis of the characteristics of the lens given by the manufacturer. The performed observations have shown that reliable measurements of light scattering can be made in the interval of angles between 5 and 175°, and that the characteristics of the lens, as given by the manufacturer, appear not to be accurate at angles close to 45 and 135°.

The design of the tested nephelometer (developed by Dr. G. W. Grams of the School of Geophysical Sciences at Georgia Tech) is depicted in Figure 1a. Figure 1b shows schematically the operating principle of the fisheye lens prototype of the nephelometer herein discussed, and Figure 2 shows the geometry of the system. This nephelometer can properly operate if the particles are uniformly mixed in the sample volume, and if they are at a concentration low enough to disregard the effect of multiple light scattering. Good uniform mixing can be obtained by reducing the sample volume to limits compatible with the

characteristics of the fisheye lens employed.

The following discussion pertains to the specific lens used during the measurements (Nikkor Orthographic Projection 10 mm f5.6); nevertheless, similar discussions can be easily extended on other cases. According to manufacturer specifications on the lens, the lens accommodates the 180° of the field of view following a formula that, for the angle $\phi = 0$, becomes (see Fig. 3):

$$x = L \sin \xi \qquad \begin{array}{l}(x \text{ in millimeters;} \\ L \text{ constant of the} \\ \text{lens - 10 mm})\end{array} \qquad (1.B)$$

where x is the distance from the intersection of the optical axis of the lens with the image focal plane (center of the image) and ξ is the angle with the optical axis. It is also stated that the radiances read on the film are proportional to the cosine of incidence. Therefore, by changing the angle from ξ to the light scattering angle θ, and by taking into account the geometry of the laser beam with θ, it follows that the lens should have the following properties:

1. The radiances measured are directly proportional to the particle phase functions. In fact, the radiance R, received in front of the lens in direction θ, is:

$$R(\theta, \phi = 0) = \sigma(\theta)/\sin \theta \qquad (2.B)$$

After the lens,

$$R(x,\ y = 0) \propto \sigma(\Theta)\cos\xi/\sin\Theta = \sigma(\Theta) \qquad (3.B)$$

2. The light scattering cross sections of the particles are directly proportional to line integrals of the measured radiances. This is because $dx = d(\cos\Theta)$, then:

$$\int_0^{\pi} \sigma(\Theta)d(\cos\Theta) \propto \int_{-L}^{-L} R(x)dx \qquad (4.B)$$

3. The half ellipsis that results on the image plane by observing a laser beam with the optical axis orthogonal to the lens - but non crossing the laser beam, as in Figure 3 - once projected on the major axis of the ellipsis will again follow the same functional dependence. The projection formula can be easily visualized as projecting maximum circles of a sphere on a plane; it follows that:

$$\begin{aligned} x &= L\cos\Theta \\ y &= -L\sin\Theta\sin\phi \end{aligned} \qquad (5.B)$$

As further consequence, we can calculate the angular resolution obtainable from the lens on the image plane:

$$\begin{aligned} dl/d\Theta &= (d\,x^2 + d\,y^2)^{\frac{1}{2}}/d\Theta \\ &= L(\sin^2\Theta + \sin^2\phi\cos^2\Theta)^{\frac{1}{2}} \end{aligned} \qquad (6.B)$$

For small values of ϕ:

$$dl/d\Theta \approx L(\sin^2\Theta+\phi^2\cos^2\Theta)^{\frac{1}{2}} \qquad (7.B)$$

That is, the resolution has a maximum for $\Theta = 90°$, and is small

for low and large scattering angles (Θ close to 0 and 180°); when the optical axis of the lens and the laser beam are perpendicular (ϕ = 0°), $dI/d\Theta = 0$ for Θ = 0 and 180°. Therefore, to obtain a good resolution at low and high light scattering angles, it is necessary to observe the image of the laser beam with some elliptical deformation on the x-y plane.

Measurements made with a prototype of the fisheye nephelometer have been carried out using a photographic camera and a microdensitometer for analyzing the films. A TSI monodisperse aerosol generator has been used for intercalibrating the prototype with the polar nephelometer. The photographic density (in the linear region of the response) is related to the received radiances by the relation:

$$R(x,y) = \alpha 10^{\gamma D(x.y)} \qquad (8.B)$$

where α and γ are constants that depend respectively on the exposure and on the type of film, and $D(x,y)$ is the film density.

We can observe now that by repeatedly scanning the image (along parallel lines very close to each other in any convenient direction), it is possible to correct the effect introduced by the angle ϕ. In particular, if each scan is the plot of the photographic density along segments (x_1, y_i - x_2, y_i, i = 1,n). The envelope of the maxima of the measured densities is directly related to the light scattering through an equation of the kind of equation 3 because the maxima are the only positions where the exposed portion on the film completely intersects the probing

beam of the densitometer. Conversely, a generic curve cannot be correlated with the light scattering properties of the particles unless the value of angle is exactly known and, therefore, the response as a function of position.

The results obtained from numerous densitometric scans in one of the measurements is reproduced in Figure 4. These measurements have been obtained with monodisperse aerosol of spherical particles of about 0.8 μm radius (size parameter about 7.9) with 75% Ammonium Sulfate and 25% Methylene Blue. The densitometer was set for a resolution of about 0.06 μm.

Figure 5 shows the curves representing the envelope of the maxima of the various curves, while in Figure 6 the densitometric data (triangles) have been digitized and reduced following Equations (5) and (8). The photographic constants α and γ have been set to fit approximately the results of the polar nephelometer (squares). The origin of the apparent differences in the position of the peaks has not yet been fully understood. They could be due to variation in the performance of the vibrating orifice generator or to non uniform distribution of particles density within the sampling volume (contained in a box about 4 m long and 50 cm x 30 cm wide).

To assess the angular performance of the lens, we have performed measurements with DOP particles of size parameter about 12 for the two orthogonal planes of polarization. Figure 7 shows the plot of the cosine of the angles of the peaks and valleys in the phase function of DOP as obtained from the measurements with the polar nephelometer versus their corresponding position in the

picture taken with the fisheye. Taking into account the fact that the polar nephelometer cannot resolve peaks and valleys in the phase functions with a precision better than 5°, we can observe that there is a slight systematic tendency of the fisheye coordinates to stay below the 45° correlation line, especially for directions around 45 and 135°.

We can conclude that the photographic measurements constitute a preliminary verification, made with a rather primitive experimental set up, that a fisheye polar nephelometer can be successfully realized on the basis of the observations and discussions herein performed. In the present configuration the system resulted to easily provide reliable measurements of the aerosol scattered light at scattering angles of 5 and 175°, with an improvement of 5° over the laboratory instrument. This feature definitively proves that the development of an actual instrument for light scattering measurements based on this principle is worthwhile to be pursued. The optical properties of the lens, as given by the manufacturer can be considered acceptable in the first approximation. A calibration should be performed on an actual system.

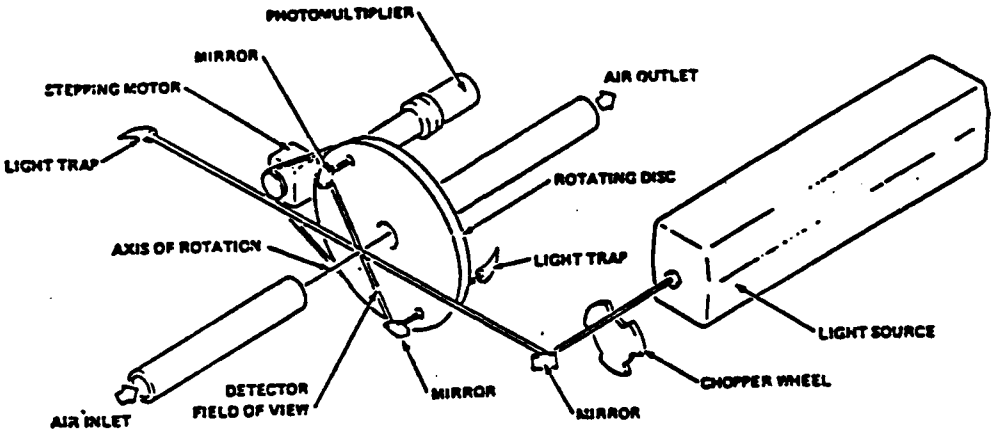

a.

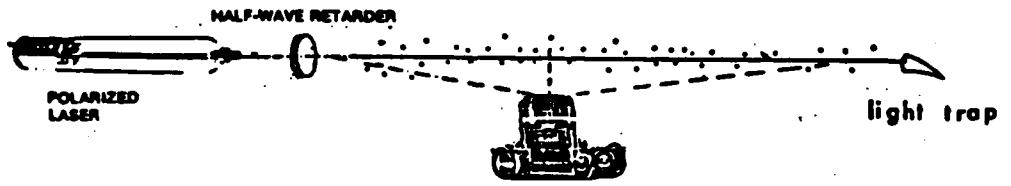

b.

Figure 1: Possible layouts for polar nephelometer: 1(a) polar nephelometer as proposed by Grams et al., 1975 (Opt. Eng., 14, 85-80); 1(b) fisheye polar nephelometer (note that in this case the scattering volume is distributed along the total portion of laser beam under observation.

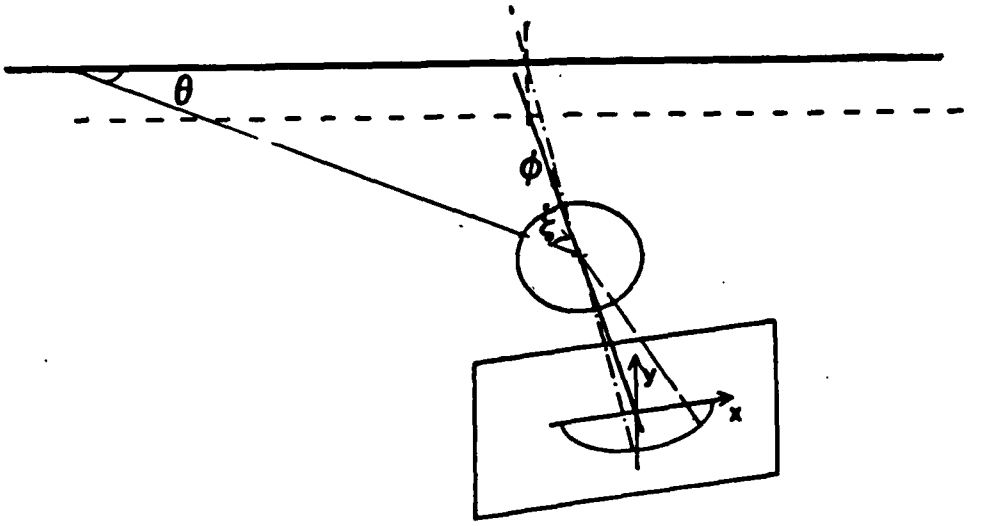

Figure 2: Geometry of the problem.

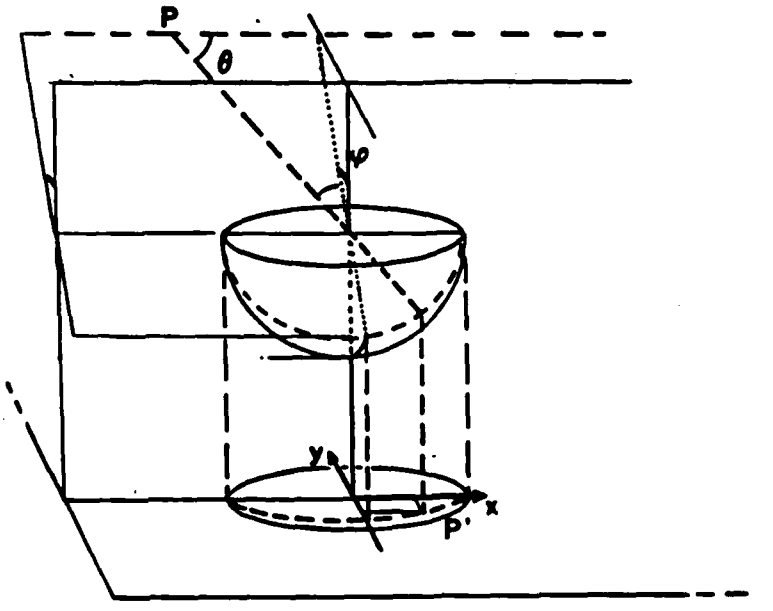

Figure 3: Geometry of the orthographic projection.

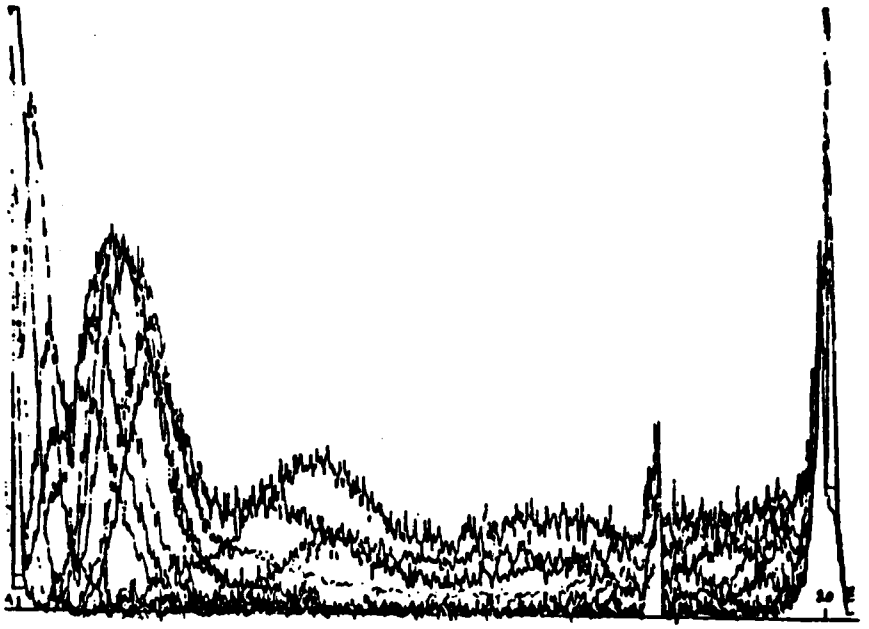

Figure 4: Sample output of the microdensitometer for 0.8 μm particles (mixture of Ammonium Sulfate and Methylene Blue).

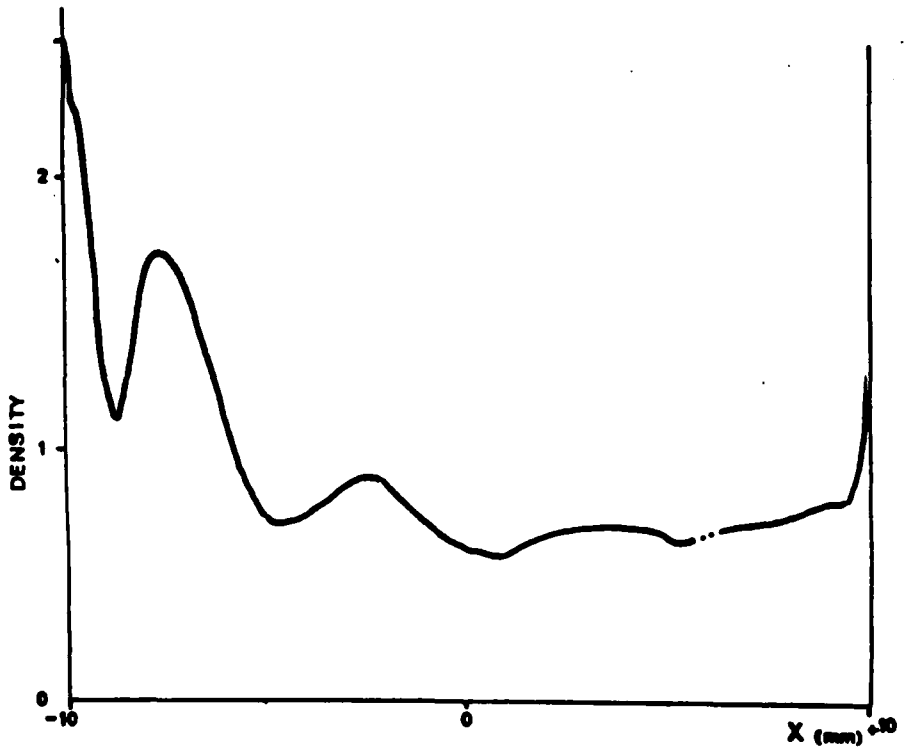

Figure 5: Same as Figure 4 after density calibration. Only the significant experimental points are reported.

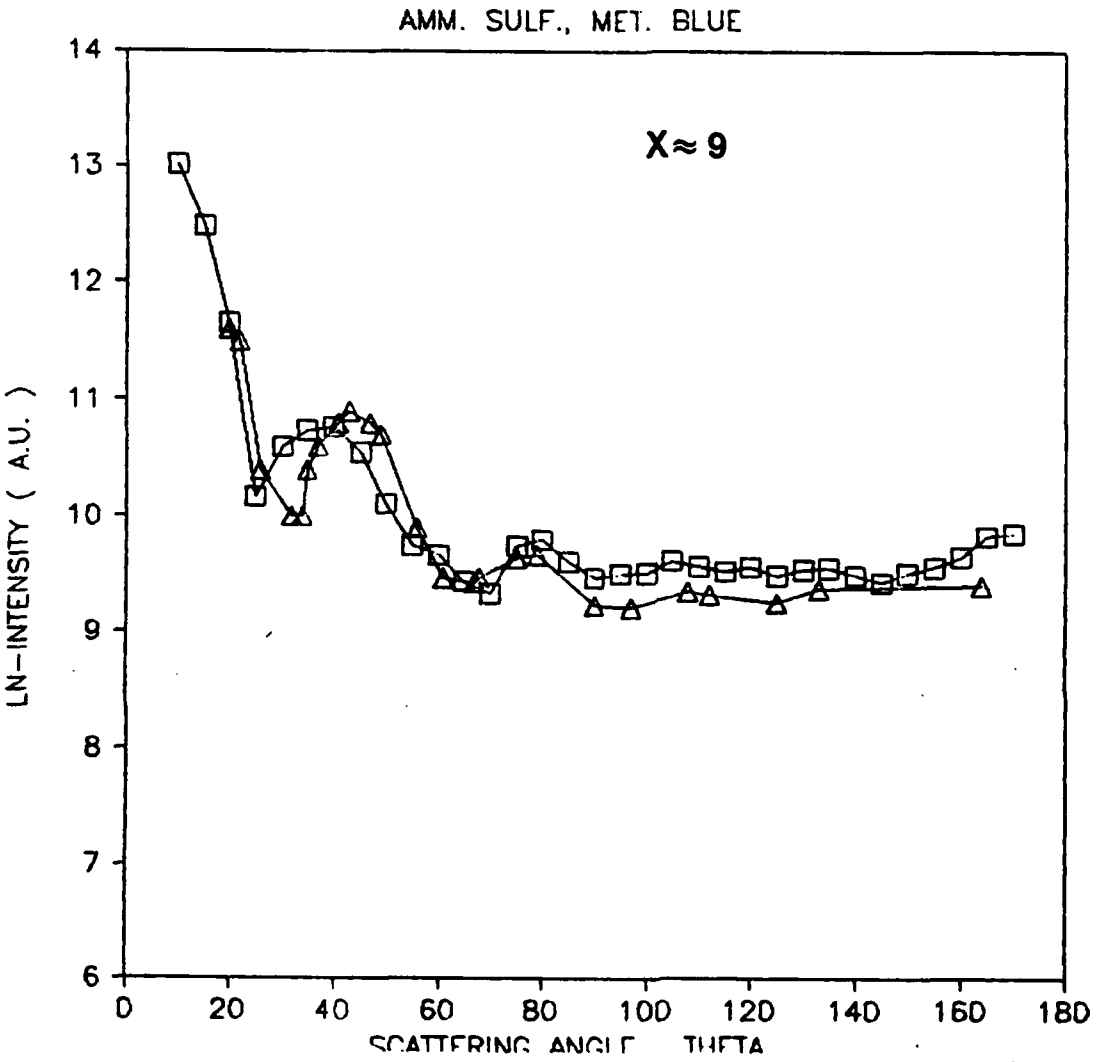

Figure 6: Intercomparison of the results obtained with the two nephelometers. (□) results from the nephelometer in Figure 1(a), (Δ) results from the fisheye nephelometer (Figure 1(b)).

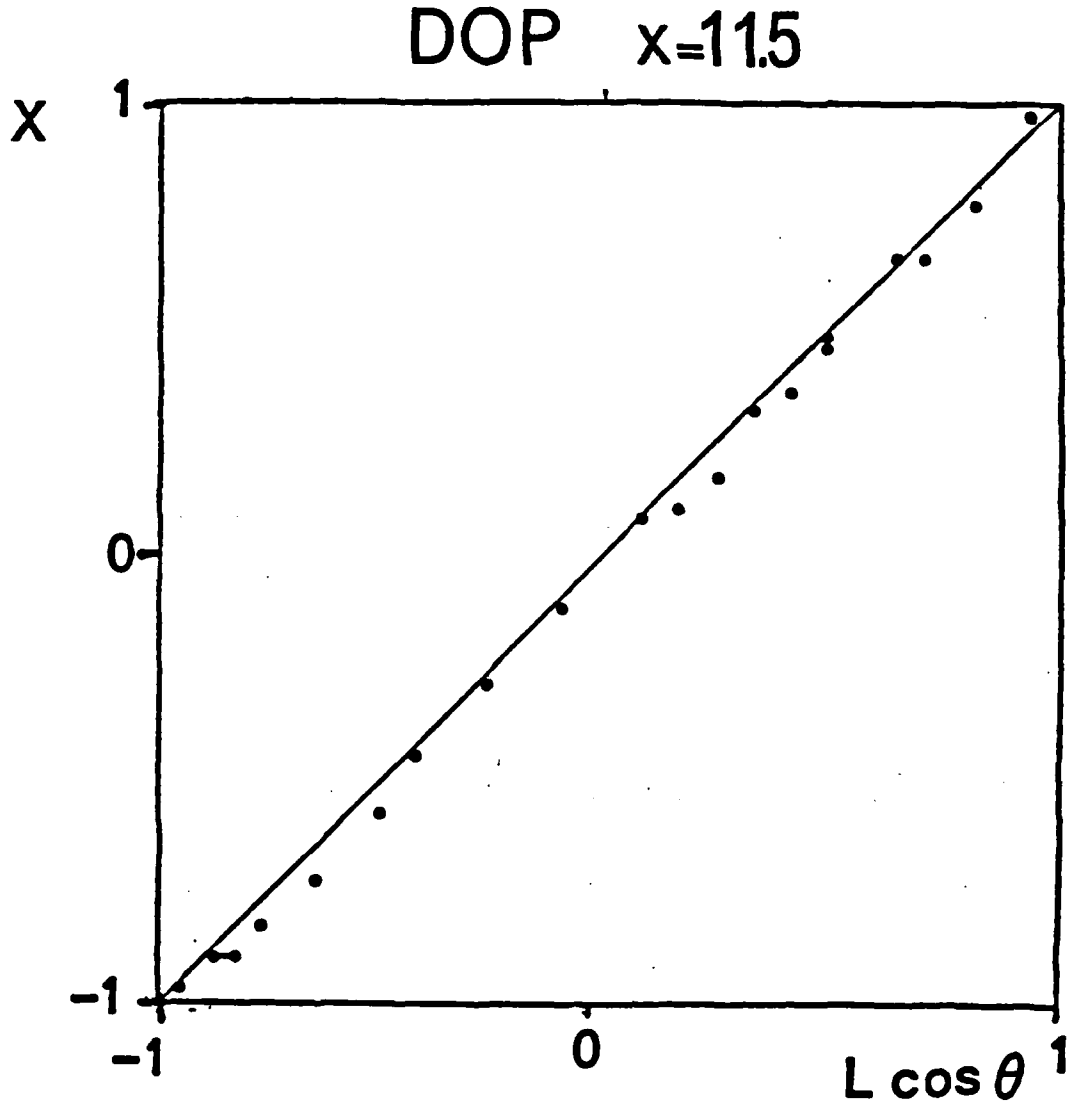

Figure 7: Correlation line between the position of the peaks and valley in the phase function of DOP monodisperse aerosol as detected by the fisheye nephelometer.

APPENDIX C

MEASURED PHASE FUNCTIONS

The angular light scattering measurements herein reported have been corrected for the effect of the scattering angle on the field of view of the detector, and for the molecular contribution to the light scattering.

We have normalized the results of angular light scattering dividing by the best possible estimate of the total light energy scattered at all angles. In fact the number density of the particles flowing in the sample volume depends on experimental parameters (such as the performance of the particle generator and the amount of air used for dispersing the particles) that can not be measured with sufficient precision to permit dependable determination of the particle cross sectional area. Therefore, we have simply divided our angular data set by the quantity:

$$\sigma = g_o = \sum_{i}^{N} w^s{}_i \, V_i^p \qquad (N=33;\ p=1.2) \qquad (1.C$$

where $w^s{}_i$ are suitable weights, V_i^p the measured values of light scattering, and p (=1,2) the index for parallel and perpendicular polarization of the incident laser light.

In order to compute the Legendre polynomial coefficients we have to take into account that the Legendre polynomial are not an orthogonal set of polynomials in the discrete space of our experimental data (33 points taken every 5° in the interval between 10 and 170°). That is the quantities:

$$\pi_{ij} = \sum_{k}^{N} P_i P_j(\mu_k) \quad (i=1,n;\ j=1,n;\ N=33;\ \mu_k=\cos\ \theta_k) \qquad (2.C$$

are different from the analytical values of the corresponding integrals:

$$\Pi_{ij} = \int_{-1}^{1} P_i P_j d\mu \qquad (3.C$$

To obtain the best estimate of the Legendre polynomial coefficients from our data, we have defined the matrix Π, with dimensions nx33 and with elements, π_{ij}, so that the equation

$$\vec{g} = \|\Pi^T \Pi\|^{-1} \|\Pi\|^T \vec{V} \qquad (4.C$$

provides the desired results in the least square sense.

In this study the optimization of the series has been performed with a trial and error method by varying the dimension n of the array of the coefficients, $\vec{g}$, and of the matrix Π. As optimum value of n has been taken the one whose associated polynomial was best fitting the measured values without exhibiting physically irrisonable oscillations in between the experimental points. Naturally, varying the order n of the polynomial, different values for the low order coefficients are found. In particular the value of the coefficient g_o, varies from the expected unitary value. This basically indicates the existing difference between the normalization constants of the experimental data and of the optimized polynomial series.

Linear inversions performed with eq 4.c are well known to produce negative and physically meaningless solutions when applied to experimental data affected by experimental errors or by insufficient angular resolution. Therefore, unconstrained analysis of this kind, when giving negative solutions, will provide a necessary (but not sufficient) indication of applications on ill conditioned cases.

The figures that follow report the angular light scattering measurements for the various aerosols studied. The triangles and the circles in the figures are respectively the experimental points for polarization of the incident light parallel and perpendicular to the plane of scattering (the crosses have no scientific content since are numbers proportional to the recovery time of the photomultiplier). The continuous lines are the fits of the experimental data computed with the Legendre polynomials. The set of Legendre polynomial coefficients for the two curves are reported underneath each figure (first column the fit for triangles, second for circles). Some of the times, a third column is present with the averages between the first two set of coefficients (unpolarized light).

In general, by observing the figures it is possible to notice that the computed polynomials fit the experimental data better in the case where the experimental phase functions have oscillations of small amplitude. This occurs in general in the case of small particles or in the case of particles with complex internal structure or shape.

In the case of small particles this is not surprising, and

the reasons have been discussed in page 7. In the case of large particles with a complex shape or internal structure, the results can be interpreted as due to the combined effect of the low angular resolution of the experiments and of the random orientation of the particles. Therefore, in our opinion, the reported polynomial coefficients in the case of these particles cannot be considered any longer an experimental estimate of a set of true coefficients that can be uniquely associated with the particles under study. Sometimes the polynomials fitting the measurements for the two polarizations of the incident light do not merge, as they should, at 0 and 180°. At this stage of the research we have performed separate fits for the two sets to better the actual applicability and versatility of the method. In fact, we did not include in our equations the fact that the two set of data are actually describing the same phase function, a feature that can be easily taken care by including in the analytical formulae the azimuthal dependence of the scattered light.

Nevertheless, this method has been chosen to show independently for the two polarizations of the incident light the few cases where the linear inversion method yields negative solutions (fig. 3a, c, e, f; 5a, b; 6a). As it is well known from the Lorenz Mie theory, this fact can be expected to occur more frequently in the case of large particles or of relatively high light absorbing particles because they are those that possibly require more terms in the Legendre polynomial series. However it can be noticed how negative coefficients never appear

for coefficients of order lower than 12, confirming the discussion presented for eq. 12 in the report.

FIGURE 1
Sodium Chloride
(50% Ethanol-50% Water)

Fig Number	Concentration	Size Parameter (X)
a	6.7×10^{-4}	12.6
b	6.2×10^{-4}	11
c	5.3×10^{-5}	7.8
d	6.3×10^{-5}	5

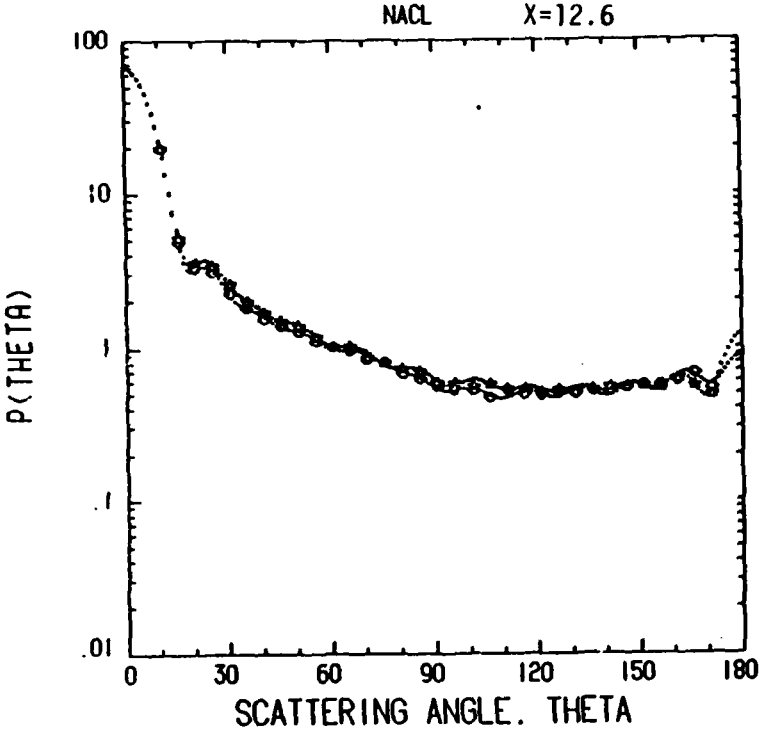

0	.1270988E 01	.1357771E 01
1	.6466732E 00	.6918252E 00
2	.5248758E 00	.5482456E 00
3	.4074316E 00	.4329281E 00
4	.3601384E 00	.3711257E 00
5	.3241526E 00	.3260231E 00
6	.3039492E 00	.3059518E 00
7	.2692437E 00	.2739699E 00
8	.2158558E 00	.2188673E 00
9	.1944480E 00	.1951364E 00
10	.2497705E 00	.2553198E 00
11	.2306771E 00	.2346123E 00
12	.1582375E 00	.1630428E 00
13	.1844484E 00	.1897511E 00
14	.1605851E 00	.1664170E 00
15	.7925063E-01	.8025742E-01
16	.6243761E-01	.6497848E-01
17	.6501001E-01	.6713444E-01
18	.5043140E-01	.5190349E-01
19	.3168091E-01	.2894255E-01
20	.2164682E-01	.2303511E-01
21	.1674466E-01	.1820778E-01
22	.1151416E-01	.1275888E-01

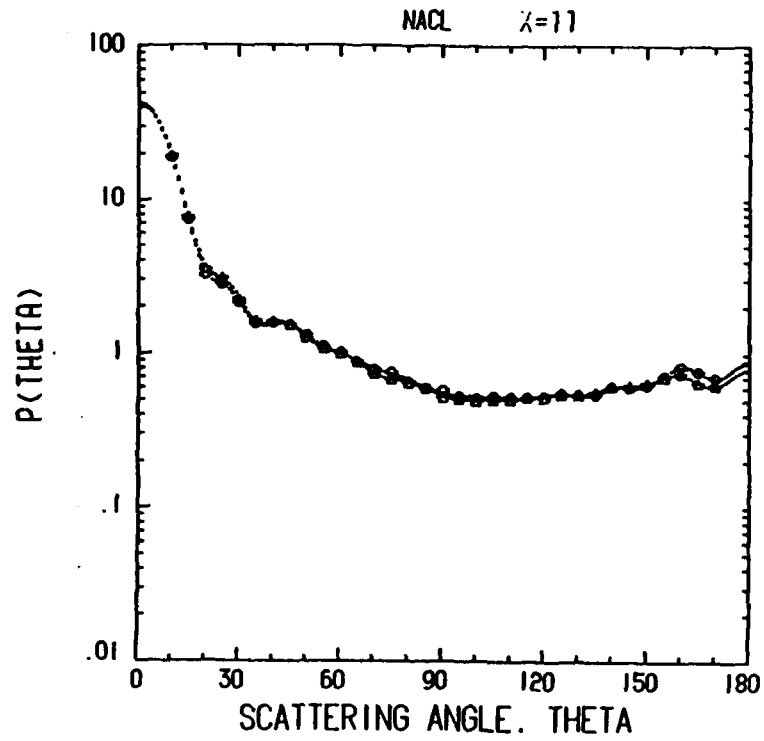

0	.1224730E 01	.1236349E 01
1	.5617428E 00	.5870272E 00
2	.4616205E 00	.4877205E 00
3	.3337274E 00	.3570063E 00
4	.2891764E 00	.2972409E 00
5	.2515317E 00	.2610124E 00
6	.2339439E 00	.2368495E 00
7	.2043363E 00	.2091489E 00
8	.1609677E 00	.1624328E 00
9	.1373961E 00	.1374613E 00
10	.1538150E 00	.1555710E 00
11	.1367059E 00	.1377237E 00
12	.8921685E-01	.9228140E-01
13	.1005978E 00	.1023464E 00
14	.8302301E-01	.8433676E-01
15	.3650256E-01	.3567655E-01
16	.2676009E-01	.2822533E-01
17	.2653040E-01	.2932477E-01
18	.1886371E-01	.2077149E-01
19	.4933590E-02	.5665172E-02
20	.2391238E-02	.1077092E-02

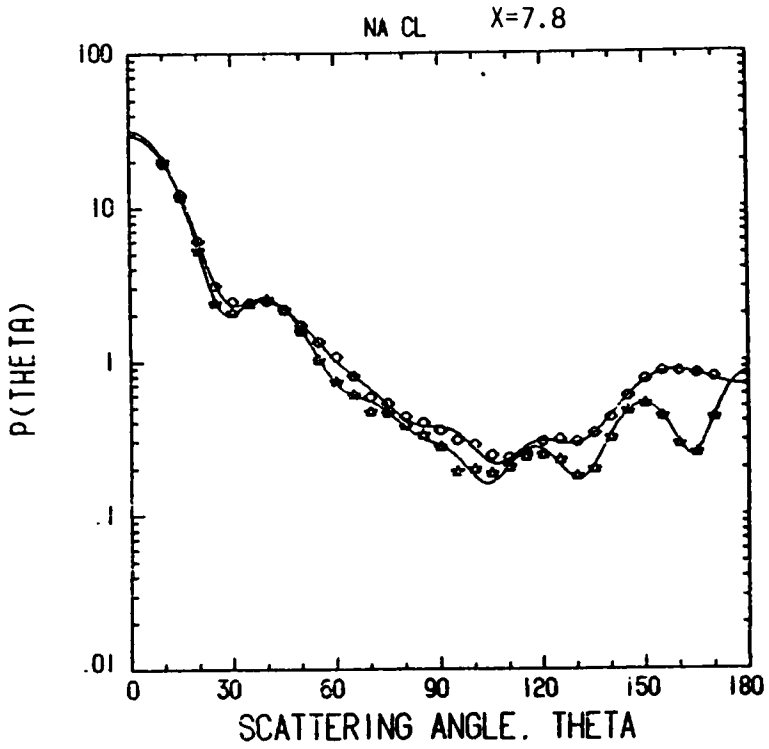

0	.1260269E 01	.1131212E 01
1	.7234176E 00	.7287620E 00
2	.5963722E 00	.5704008E 00
3	.3570141E 00	.3797069E 00
4	.2991785E 00	.2965265E 00
5	.2414891E 00	.2481529E 00
6	.2110739E 00	.2169995E 00
7	.1930304E 00	.2017772E 00
8	.1499976E 00	.1704628E 00
9	.1199753E 00	.1419548E 00
10	.8478773E-01	.1138965E 00
11	.6091657E-01	.8879634E-01
12	.3351216E-01	.4462314E-01
13	.1856563E-01	.1936515E-01
14	.8627497E-02	.1256028E-01

1c

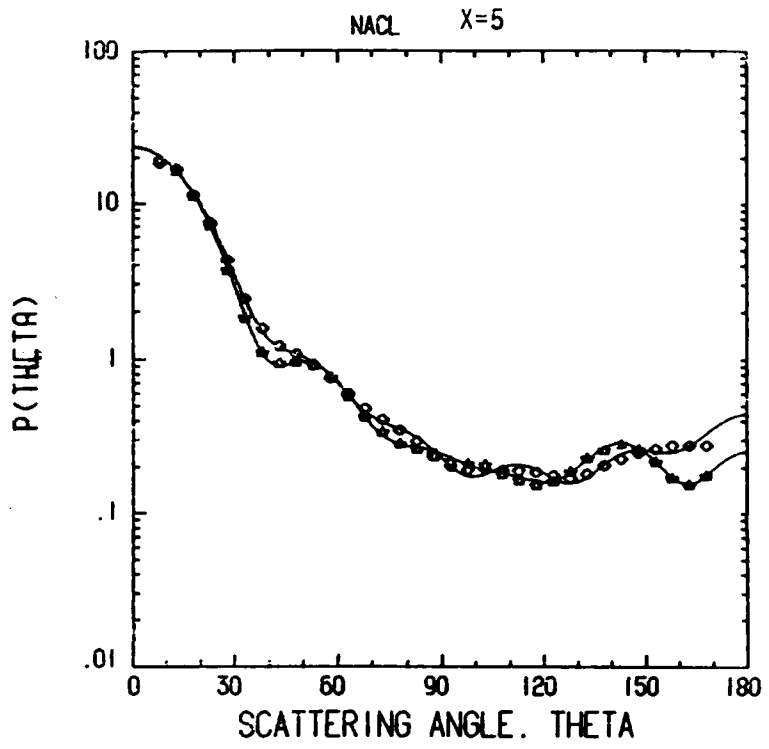

0	.1143087E 01	.1078267E 01
1	.8158811E 00	.7714379E 00
2	.6528135E 00	.6236970E 00
3	.4796871E 00	.4788631E 00
4	.3697597E 00	.3691392E 00
5	.2732807E 00	.2894102E 00
6	.1975273E 00	.2087737E 00
7	.1301190E 00	.1464311E 00
8	.7746959E-01	.8681643E-01
9	.3976598E-01	.3818191E-01
10	.1632040E-01	.1438748E-01

1d

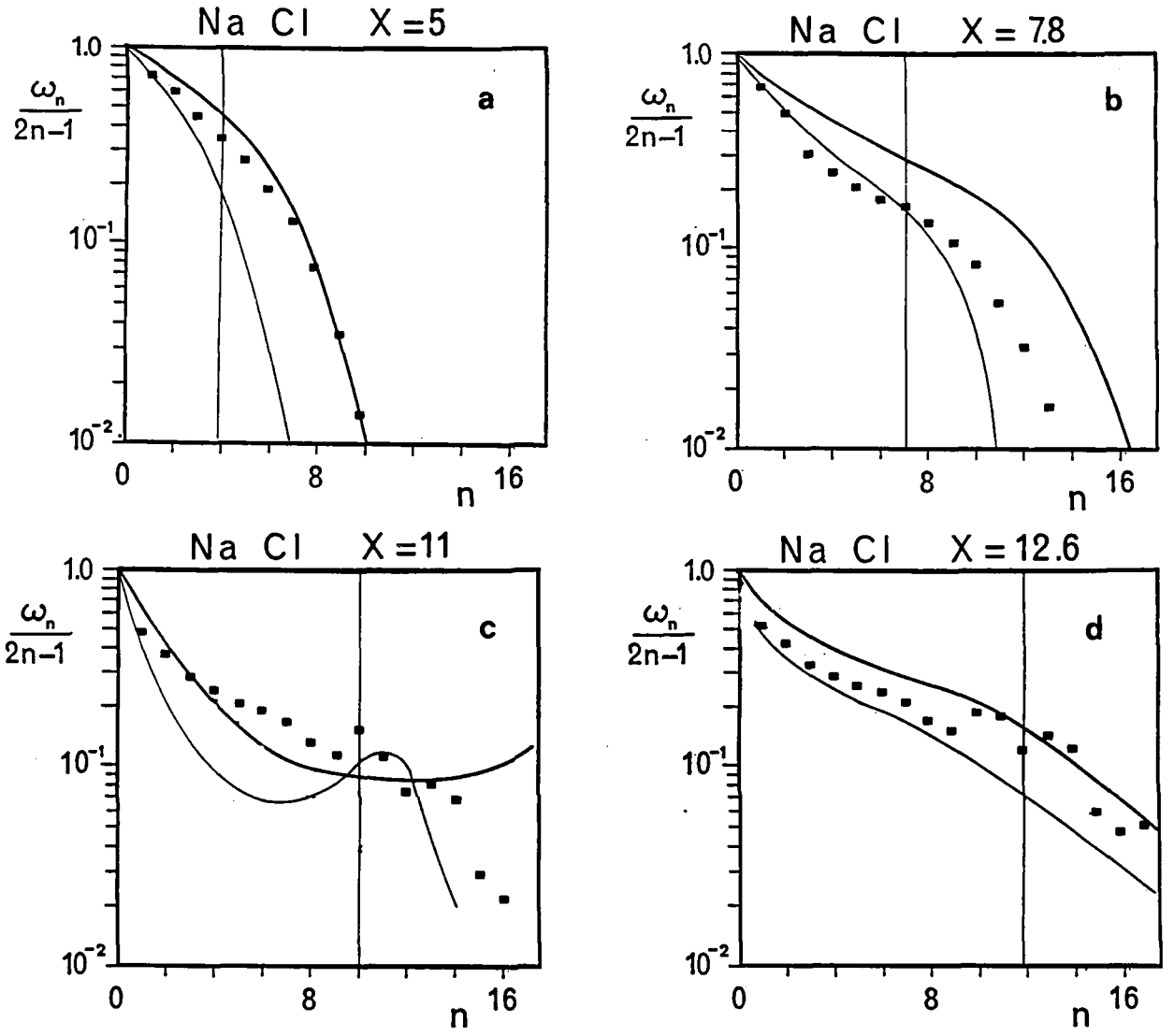

Fig. 2 - Legendre polynomial coefficients estimated from the measurements in Fig. 1 for unpolarized light (squares). The upper curves delineate the general behavior of the coefficients computed with the Lorenz Mie theory for the refractive index m=1.54; the lower curves are for m=1.3; the vertical lines are traced for m=x-1/2 (grazing incident rays).

FIGURE 3
Nigrosine Dye (75%)-Ammonium Sulfate (25%)
(75% Methanol-25% Water)

Fig Number	Concentration	Size Parameter (X)
a	$Co=8.5x10^{-4}$	8.7
b	Co/2	8.2
c	Co/4	8.1
d	Co/8	7.9
e	Co/16	6.2
f	Co/64	6.4
g	Co/128	3.9

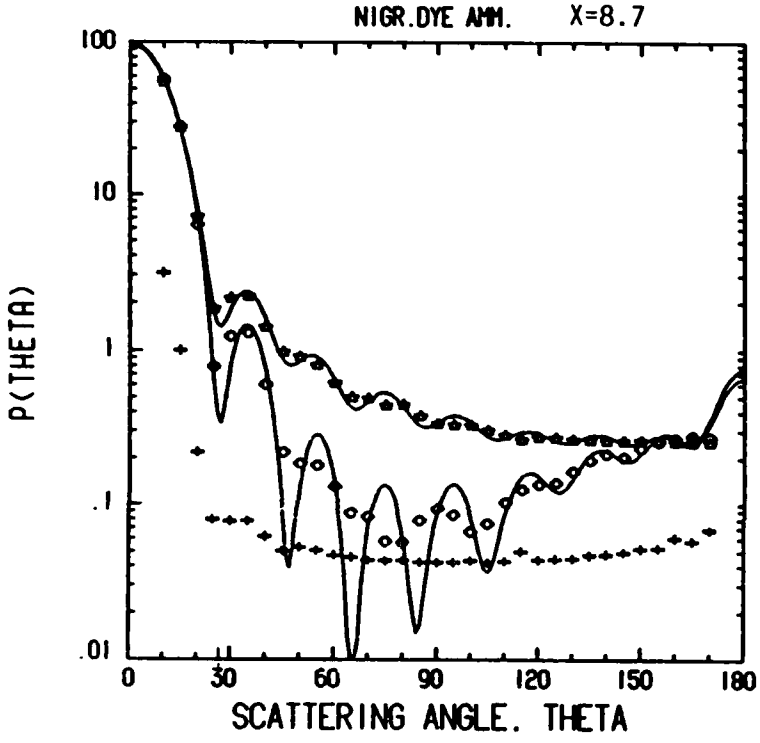

0	1.4307070	1.7372480	1.6839780
1	1.2460380	1.3484070	1.2972220
2	1.2120550	1.1903830	1.2016190
3	1.0888860	1.0470200	1.0879530
4	.9844947	.9288089	.9571614
5	.8715617	.8187808	.8451810
6	.7668216	.7200009	.7433109
7	.6486420	.6068993	.6268206
8	.5069201	.4761646	.4925469
9	.3950778	.3713308	.3832043
10	.3001685	.2856592	.2779139
11	.3208524	.2980803	.3094663
12	.2003818	.1840026	.1924071
13	.1749733	.1621703	.1686718
14	.1063446	.0988350	.1025898
15	-.0024112	-.0032198	-.0028154
16	-.0170890	-.0204435	-.0187662
17	-.0079861	-.0090169	-.0085015

3a

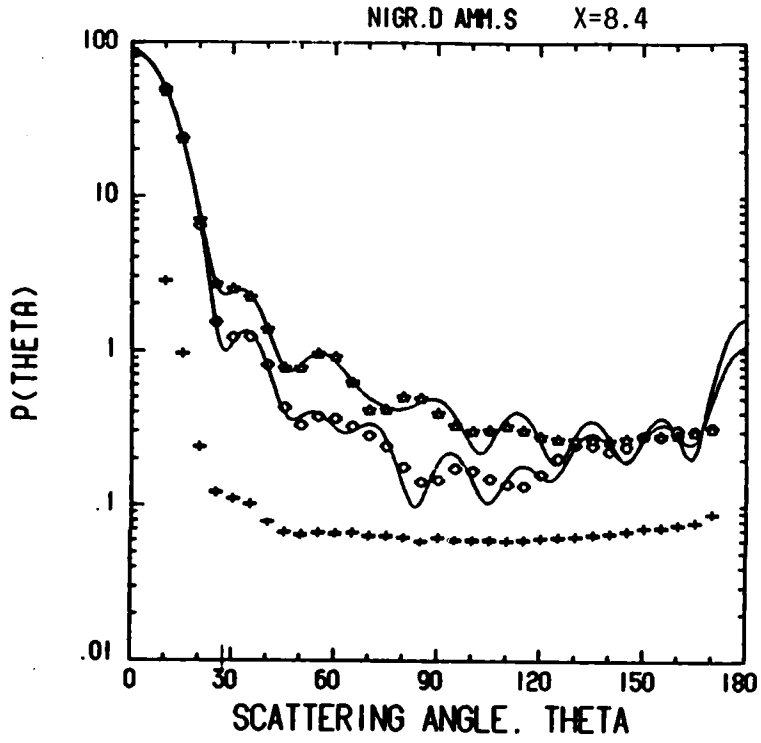

0	1.3846330	1.6436390	1.5143360
1	1.1252490	1.2238180	1.1745620
2	1.0657130	1.0683800	1.0670460
3	.9389278	.9193221	.9291248
4	.8518956	.8216661	.8367805
5	.7512050	.7087474	.7299758
6	.6574754	.6194859	.6384802
7	.5519804	.5182984	.5351391
8	.4363132	.4070432	.4216782
9	.3340988	.3017628	.3182398
10	.3368888	.3157770	.3263329
11	.2709694	.2628175	.2669435
12	.1733203	.1767907	.1750555
13	.1521108	.1601525	.1561316
14	.0994269	.0985631	.0989950
15	.0075462	-.0035674	.0019894

3b

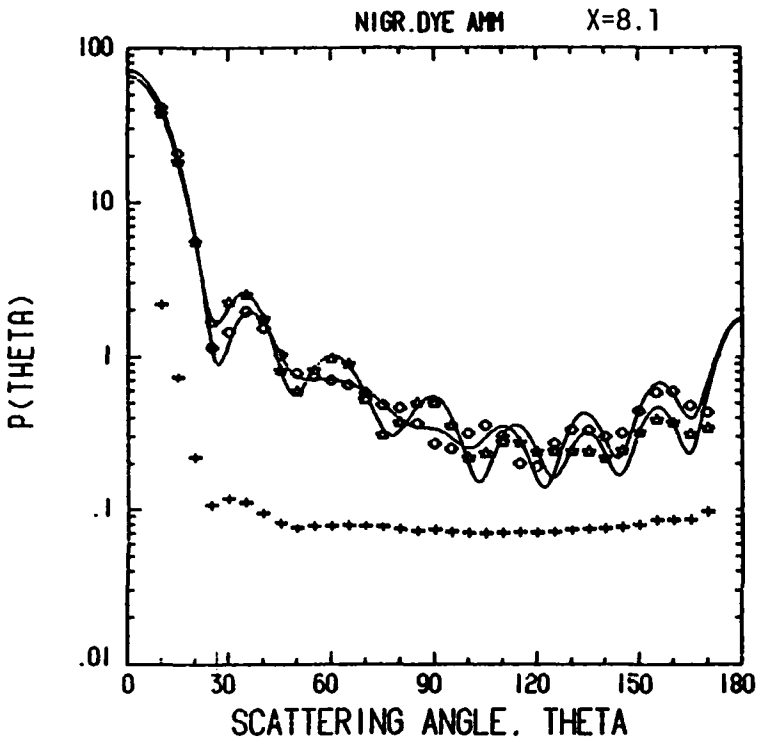

0	1.4349300	1.3977680	1.4183480
1	1.0080780	.9904728	.9992752
2	.9105606	.8435224	.8770413
3	.7528008	.6959317	.7243082
4	.6953984	.6293113	.6623545
5	.6048392	.5377716	.5713053
6	.5400553	.4756347	.5078449
7	.4651923	.4061607	.4356765
8	.3690454	.3241349	.3465901
9	.2818986	.2367808	.2593397
10	.2841692	.2507465	.2674578
11	.2261395	.2203452	.2242423
12	.1379965	.1516706	.1448336
13	.1153547	.1190438	.1171992
14	.0686598	.0586789	.0636693
15	-.0150129	-.0199116	-.0174622

3c

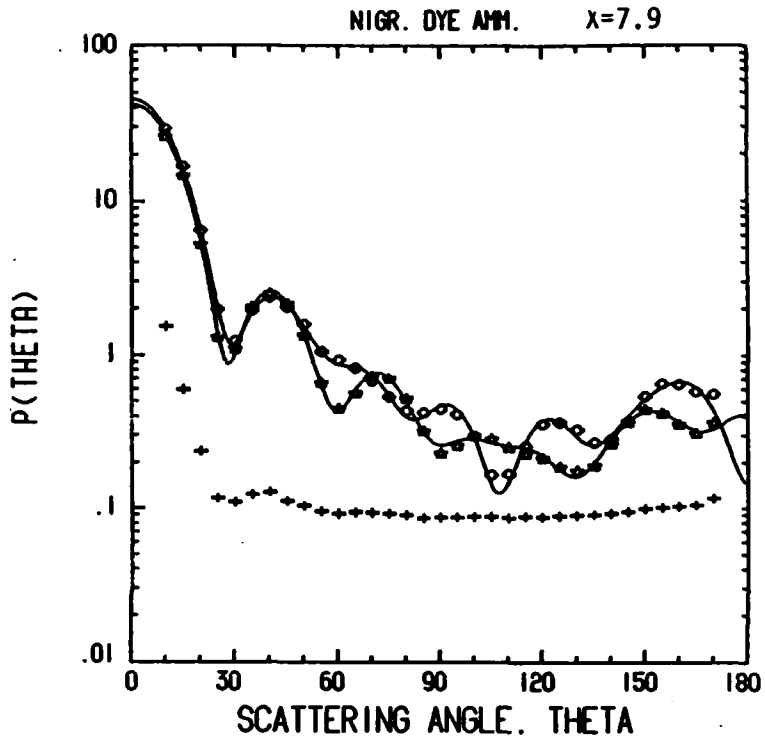

0	1.3509930	1.1949680	1.2729810
1	.8714603	.7988136	.8341365
2	.7140819	.6340216	.6745014
3	.5272310	.4782626	.5027466
4	.4602742	.4117166	.4359956
5	.4028166	.3538707	.3783436
6	.3547658	.3093714	.3320636
7	.3145193	.2815643	.2980418
8	.2810404	.2405272	.2507838
9	.2074817	.2104647	.2089732
10	.1458021	.1700871	.1579446
11	.1126837	.1068933	.1097885
12	.0586011	.0496273	.0541142
13	.0258988	.0209348	.0234173
14	.0087242	.0100747	.0083934

3d

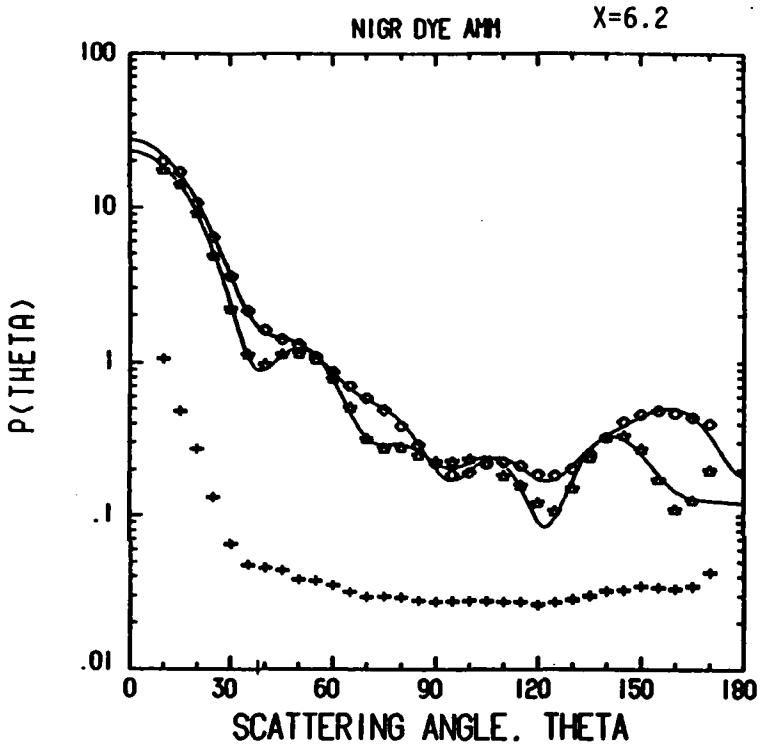

0	1.3097780	1.0353870	1.1725830
1	.9051781	.7328847	.8190212
2	.7356170	.5822515	.6589341
3	.5203477	.4411604	.4807541
4	.4062657	.3433502	.3758079
5	.3159356	.2709623	.2974489
6	.2296822	.2094884	.2195853
7	.1637572	.1629124	.1633348
8	.0932736	.0982347	.0957541
9	.0563170	.0431375	.0497273
10	.0242054	.0157789	.0199921
11	.0044508	-.0067749	-.0011620
12	-.0038432	-.0071051	-.0054742

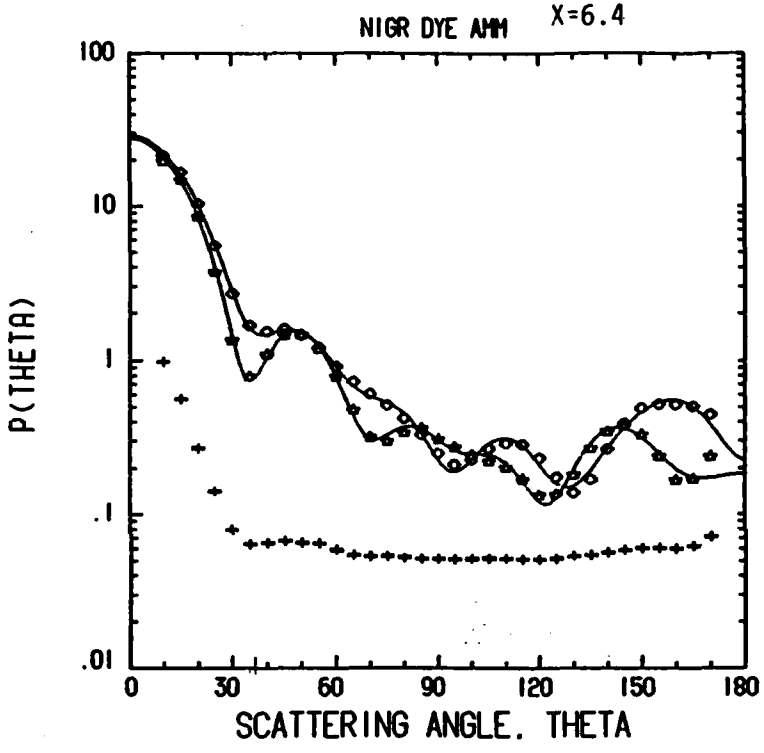

0	1.3021580	1.0818690	1.1920230
1	.8810278	.7409315	.8109794
2	.7093597	.5911627	.6502609
3	.5073787	.4512666	.4793227
4	.4149545	.3679761	.3914652
5	.3268970	.3137386	.3203178
6	.2599168	.2520384	.2559776
7	.1971071	.2152078	.2061574
8	.1193710	.1517450	.1355579
9	.0800995	.0854297	.0827646
10	.0352750	.0393203	.0372976
11	.0069078	.0037923	.0053501
12	-.0030528	-.0030047	-.0030288

3e

3f

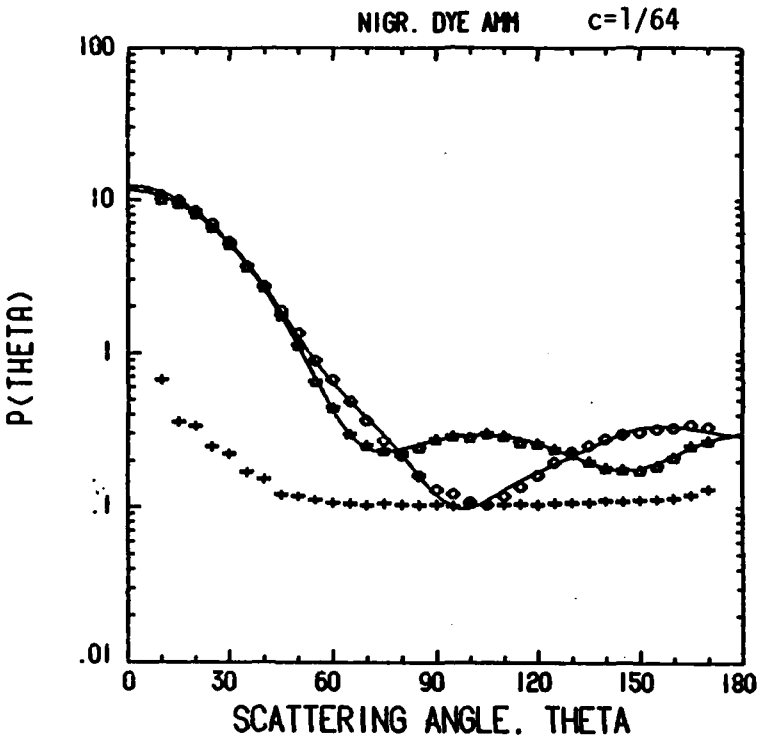

0	1.1094020	1.0883350	1.0888680
1	.7726784	.7211771	.7468277
2	.5899336	.5361547	.5630441
3	.3459422	.3571302	.3515362
4	.1929048	.1955321	.1942185
5	.1000879	.0785551	.0893215
6	.0403279	.0296997	.0350138
7	.0120742	.0063206	.0091974
8	-.0002078	.0012250	.0005086

FIGURE 4
Chlorauric Acid-Sodium Citrate
(Prepared as in Ref 3A and diluted
in 50% Ethanol-50% Water)

Fig Number	Concentration ($Co=5.5x10^{-4}$)	Size Parameter (X)
a	Co/4	9
b	Co/8	6.7
c	Co/16	6.7

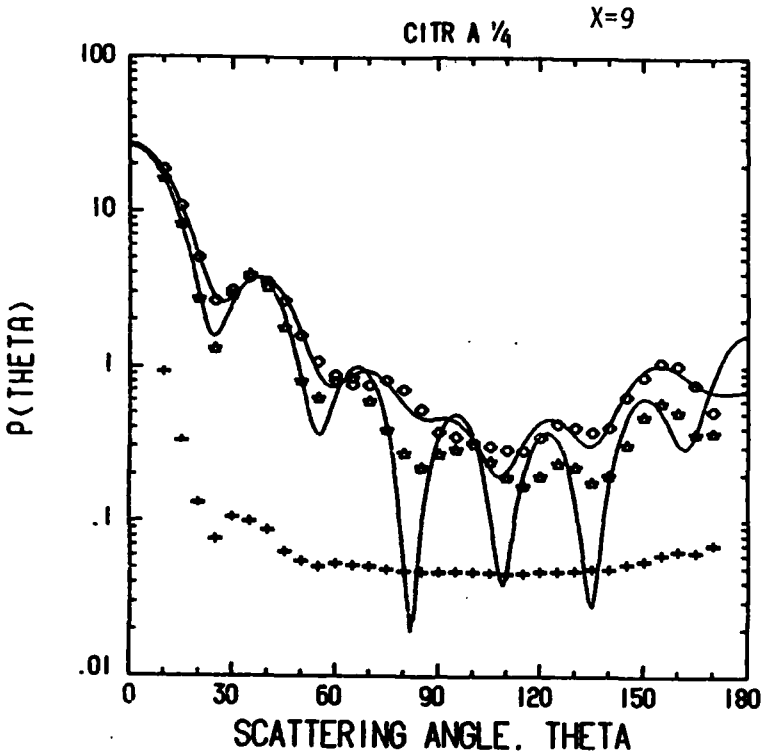

0	1.8813940	1.0118120
1	.7142778	.6078148
2	.5082573	.4683148
3	.3170278	.2753144
4	.2504410	.2128177
5	.1889540	.1467190
6	.1505694	.1387166
7	.1504518	.1311170
8	.1387419	.1316130
9	.1481431	.1324136
10	.1073003	.1318192
11	.0772988	.1088120
12	.0393368	.0747156

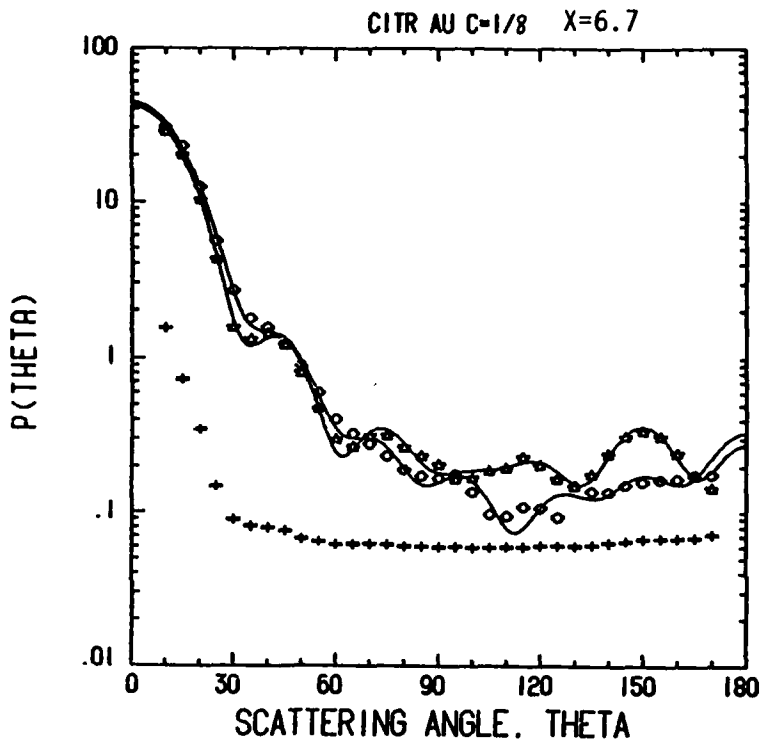

0	1.3390240	1.2276140
1	1.0977390	.9337705
2	.9356620	.8176196
3	.7640380	.6713103
4	.6122978	.5536182
5	.4846846	.4512173
6	.3783839	.3571155
7	.2893140	.2855194
8	.2131522	.2116127
9	.1425555	.1565100
10	.0874502	.0982182
11	.0444824	.0464196
12	.0159282	.0185196

4b

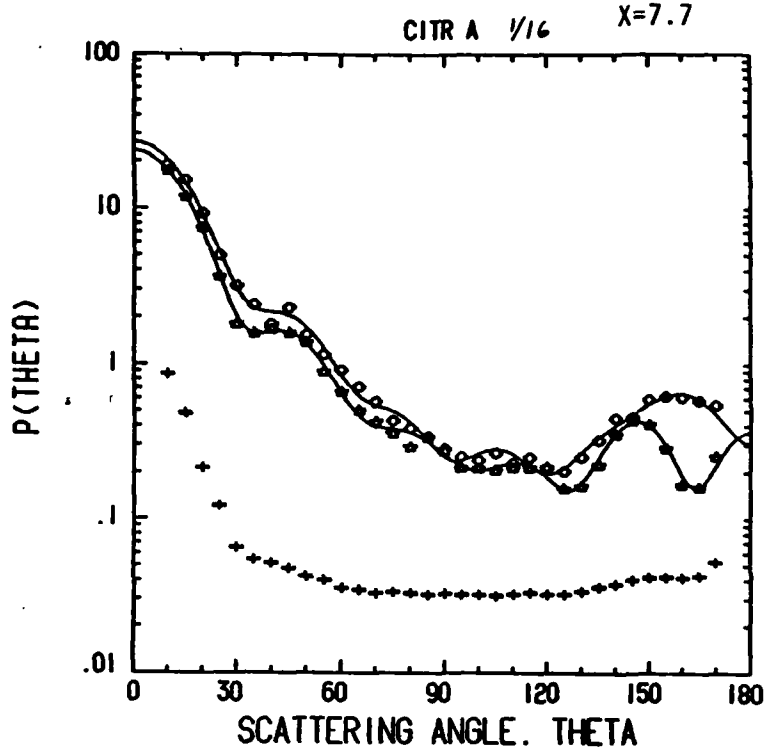

0	1.3110380	1.0263140
1	.8437932	.6765194
2	.6828863	.5320199
3	.4507037	.3609129
4	.3476301	.2918199
5	.2672963	.2384230
6	.2076018	.1850781
7	.1721897	.1586140
8	.1177190	.1154178
9	.0823403	.0784571
10	.0438189	.0473108
11	.0164662	.0128154
12	-.0006231	.0071156

4c

FIGURE 5
Chlorauric Acid-Citric Acid
(Prepared as in Ref 3A and diluted
in 50% Ethanol-50% Water)

Fig Number	Concentration ($Co=4.3x10^{-4}$)	Size Parameter (X)
a	Co/2	x=9
b	Co/4	x=6.7

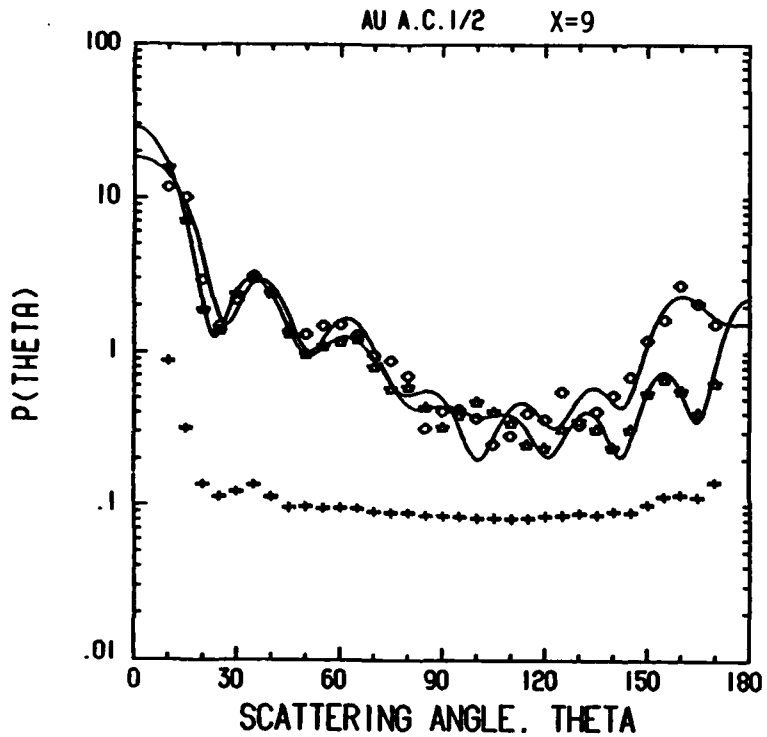

0	1.2424140	1.0698350	1.1561240
1	.4737827	.5501645	.5119781
2	.4652936	.3995777	.4324356
3	.1551410	.2368372	.1959891
4	.2125302	.2179666	.2152483
5	.1467236	.1746235	.1606735
6	.1585485	.1743645	.1664565
7	.1381020	.1566073	.1473546
8	.0932286	.1230513	.1081399
9	.0776910	.0974478	.0875694
10	.0476903	.1367774	.0922338
11	.0748355	.1247444	.0997900
12	.0283537	.0852971	.0568253
13	.0139656	.0588255	.0363956
14	-.0327032	.0376923	.0024945
15	-.0455878	-.0209612	-.0332745

5a

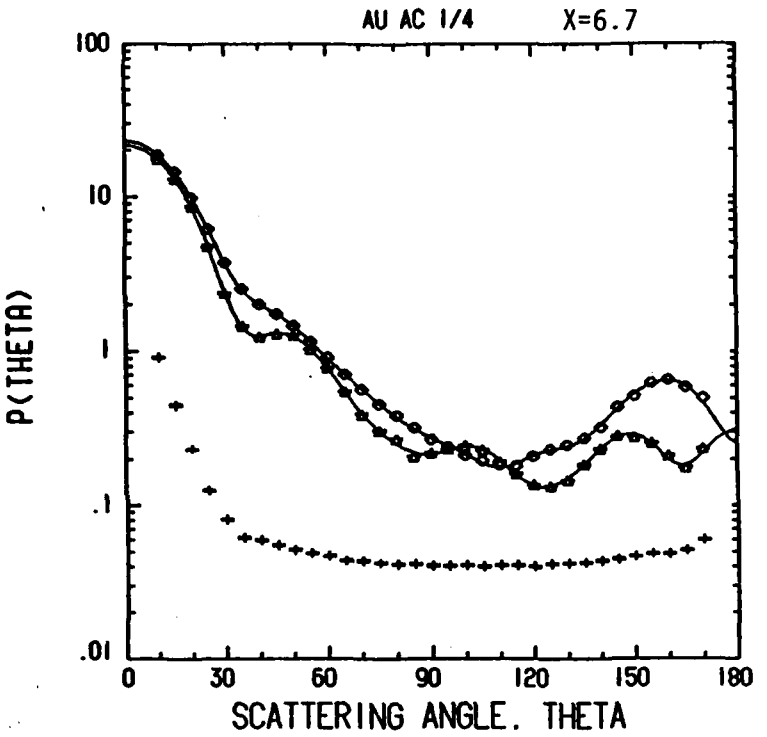

0	1.2841710	1.0266310	1.1554010
1	.8452822	.7170115	.7811466
2	.6819952	.5610927	.6215439
3	.4452043	.4087053	.4269548
4	.3407763	.3153988	.3280876
5	.2508051	.2406636	.2457344
6	.1793945	.1917498	.1855721
7	.1321128	.1482947	.1402037
8	.0799750	.0916873	.0858311
9	.0515436	.0479945	.0497690
10	.0171840	.0188747	.0180293
11	.0064208	-.0016956	.0023671
12	-.0019603	-.0040841	-.0030222
13	-.0047463	-.0072898	-.0060180
14	-.0040427	-.0027409	-.0033918

5b

FIGURE 6
Silver Nitrate-Sodium Borohydrade
(Prepared as in Ref 2A and diluted
in 50% Ethanol-50% Water)

Fig Number	Concentration ($Co=8x10^{-4}$)	Size Parameter (X)
a	Co/2	13
b	Co/4	11
c	Co/8	-
d	Co/8	9
e	Co/32	6
f	Co/64	5.4

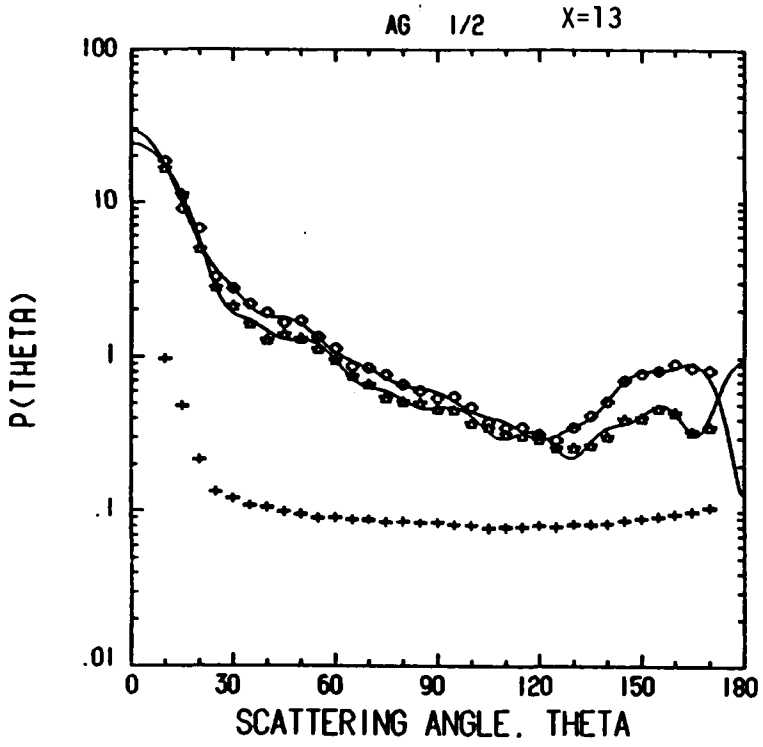

0	1.2622290	1.0756420	1.1689350
1	.6384484	.6079251	.6231866
2	.5005535	.4552236	.4778885
3	.3127261	.3281528	.3204395
4	.2821932	.2831783	.2826858
5	.2290091	.2350913	.2290502
6	.1775118	.1976377	.1875748
7	.1656750	.1618654	.1637702
8	.1159583	.1177539	.1168561
9	.0948693	.0819208	.0883950
10	.0847808	.0630637	.0739222
11	.0719454	.0416475	.0567964
12	.0438510	.0278823	.0358667
13	.0481902	.0156226	.0319064
14	.0346266	.0100090	.0224178
15	.0153685	-.0048335	.0052675
16	.0078410	-.0078078	-.0000834
17	.0090770	-.0098401	-.0003816

6a

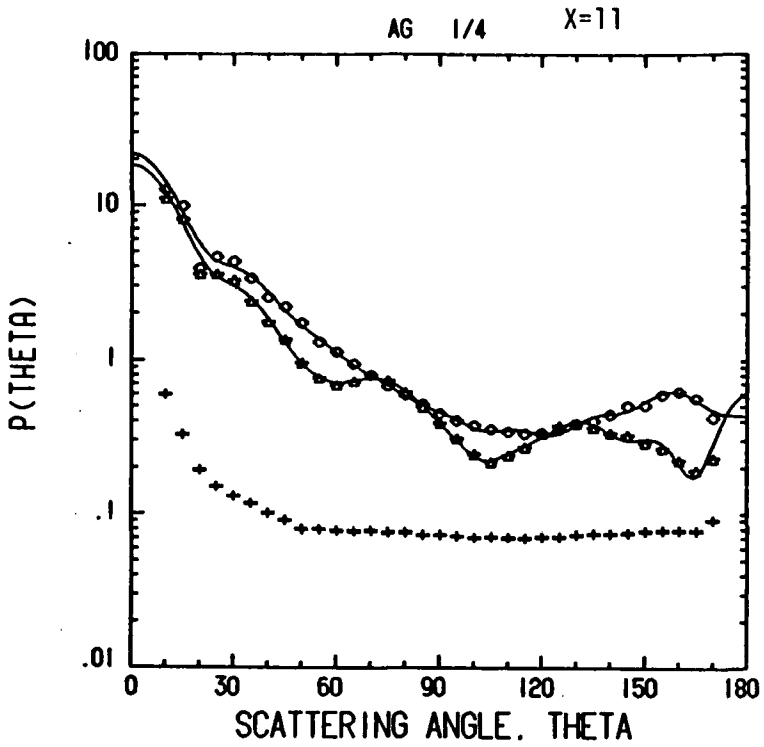

0	1.2732580	.9820459	1.1276510
1	.7018417	.5491199	.6254807
2	.5014604	.3829134	.4421869
3	.2918409	.2598713	.2758561
4	.2027745	.1897533	.1962639
5	.1471287	.1550429	.1510858
6	.1097659	.1025195	.1061527
7	.0957843	.0661184	.0809513
8	.0720455	.0596269	.0658361
9	.0617997	.0528115	.0573055
10	.0644634	.0592107	.0618370
11	.0580905	.0468664	.0524784
12	.0352233	.0301609	.0326921
13	.0343067	.0246365	.0294716
14	.0201536	.0190004	.0195770

6b

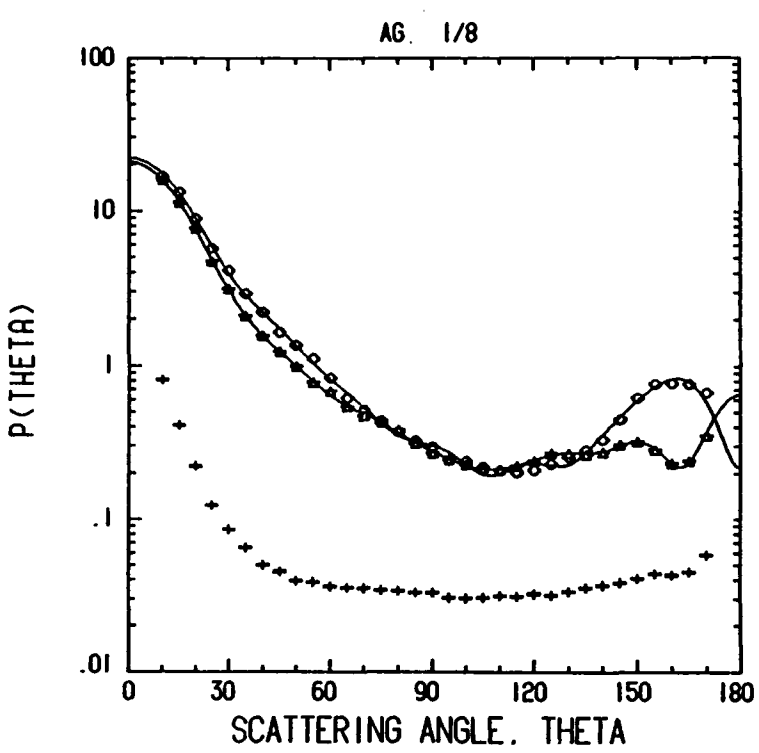

0	1.2550130	1.0391560	1.1470840
1	.7944593	.6762758	.7353673
2	.6551571	.5325792	.5938678
3	.4109398	.3814135	.3961766
4	.3140013	.2847528	.2993770
5	.2158327	.2132416	.2145371
6	.1519582	.1536075	.1527829
7	.1153046	.1053661	.1103354
8	.0703288	.0730470	.0716879
9	.0523264	.0462130	.0492697
10	.0242535	.0341308	.0291921
11	.0202121	.0179247	.0190684
12	.0070646	.0120144	.0095395
13	.0045153	.0053695	.0049424
14	-.0017862	.0065996	.0024057

6c

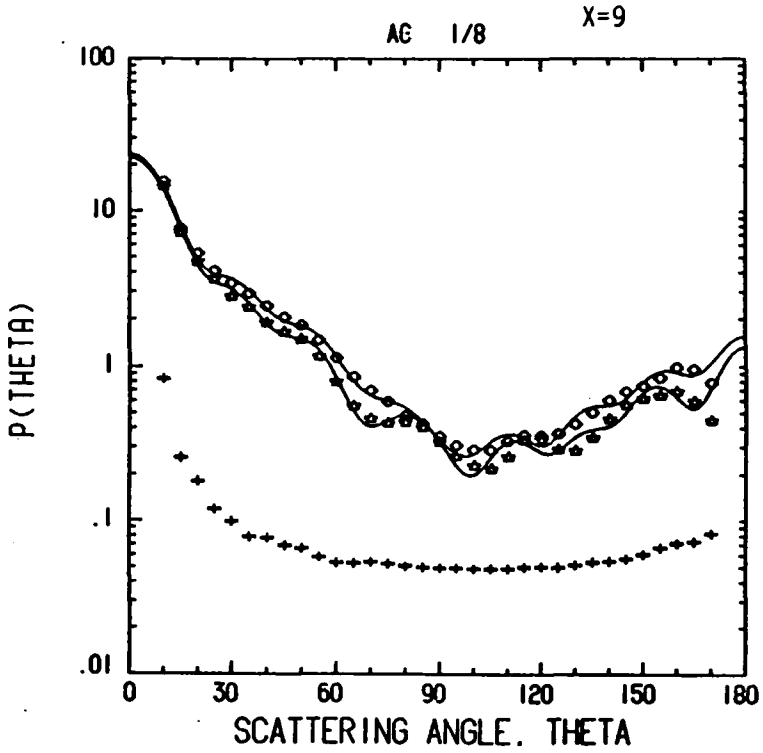

0	1.2419480	1.0302300	1.1460890
1	.6249478	.5611858	.5930667
2	.5129678	.4600948	.4865313
3	.2598811	.2637999	.2618405
4	.2004831	.2009692	.2007261
5	.1479529	.1480086	.1479807
6	.1302613	.1238260	.1270536
7	.1116191	.1092046	.1104118
8	.0821905	.0804310	.0813108
9	.0638064	.0649009	.0643536
10	.0763086	.0704293	.0733689
11	.0622761	.0527010	.0574885
12	.0436993	.0428534	.0432763
13	.0502387	.0469124	.0485756
14	.0395352	.0394233	.0394793

6d

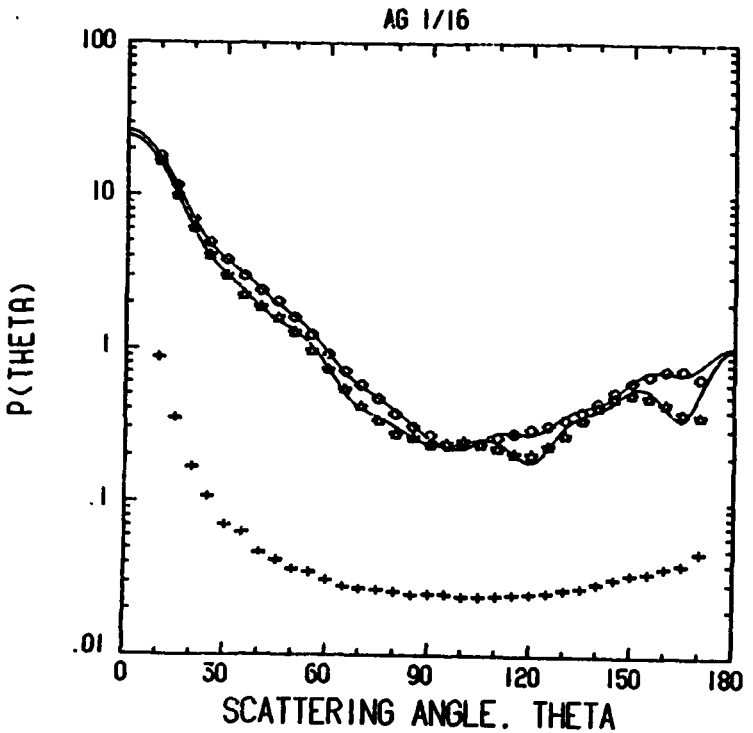

0	1.2722280	1.0609770	1.1666020
1	.7601261	.6480627	.7040944
2	.6278347	.5367610	.5822978
3	.3812084	.3496216	.3654150
4	.2852972	.2623780	.2738376
5	.2102357	.2010995	.2056676
6	.1704048	.1580564	.1642306
7	.1366556	.1351145	.1358851
8	.0998389	.0961380	.0979884
9	.0757563	.0671714	.0714638
10	.0696939	.0683070	.0690004
11	.0521842	.0469253	.0495547
12	.0324856	.0323026	.0323941
13	.0304891	.0288152	.0296522
14	.0227849	.0257134	.0242491

6e

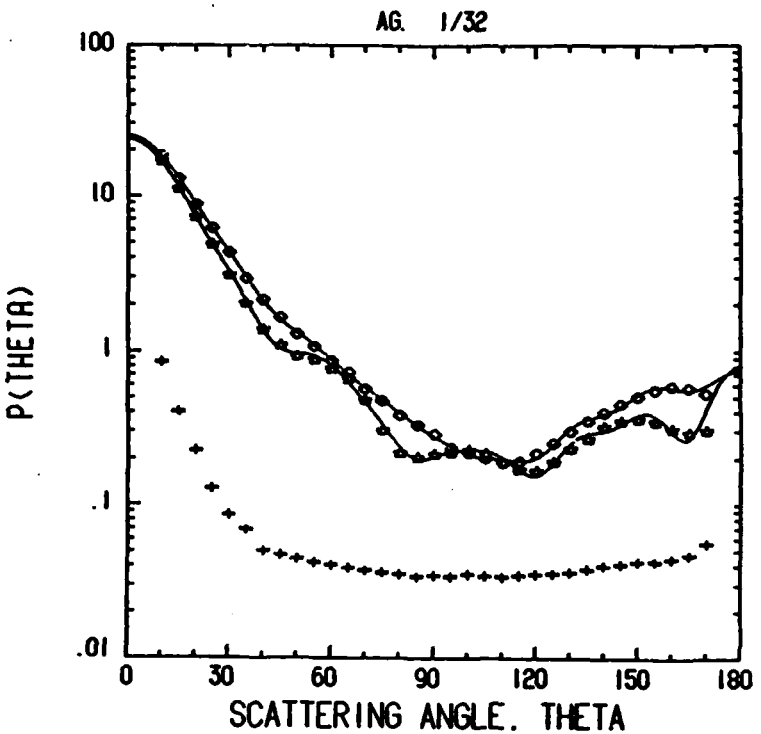

0	1.2845230	1.0391800	1.1618510
1	.8277121	.6876566	.7576342
2	.6711178	.5586388	.6148782
3	.4326368	.3892034	.4109201
4	.3249193	.2978851	.3114522
5	.2344201	.2283585	.2313893
6	.1642641	.1723675	.1683158
7	.1165178	.1264241	.1214709
8	.0745683	.0760821	.0753251
9	.0482913	.0422839	.0452876
10	.0422514	.0465233	.0443873
11	.0325256	.0356632	.0341044
12	.0200220	.0257863	.0229041
13	.0190540	.0224372	.0207456
14	.0142955	.0191767	.0167361

6f

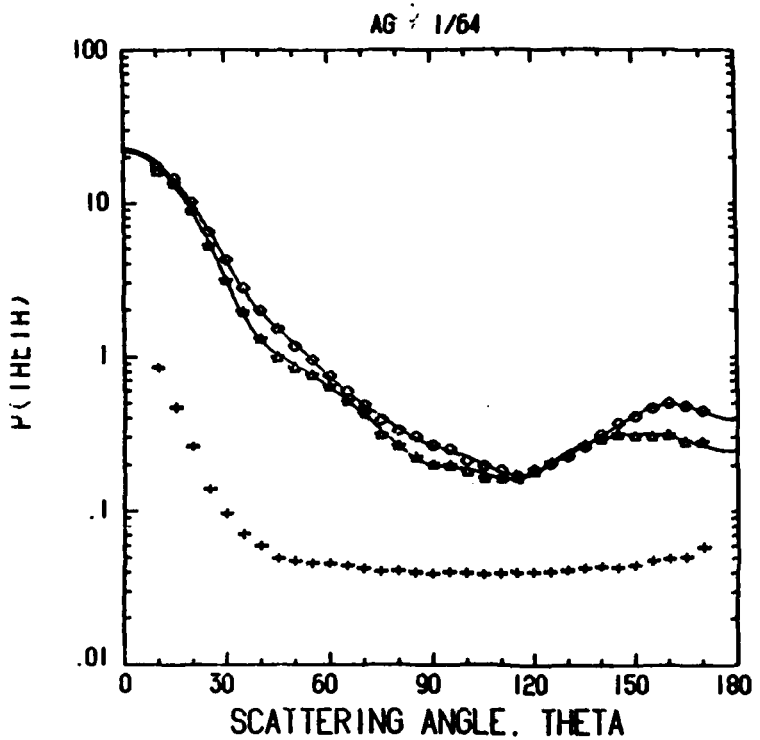

0	1.2560150	1.0552450	1.1551300
1	.6549582	.7300469	.7925024
2	.6912504	.6010921	.6461711
3	.4699264	.4380270	.4539767
4	.3503330	.3318548	.3410939
5	.2453908	.2555502	.2494705
6	.1657307	.1775371	.1716338
7	.1135735	.1215134	.1175434
8	.0676183	.0728707	.0702445
9	.0390286	.0388784	.0389535
10	.0178585	.0192748	.0185667
11	.0083361	.0084900	.0084130
12	.0015141	.0019083	.0017112

END

5-87

DTIC